Dear Dr. Jöckel,

Thank you very much for serving as an editor for my manuscript acp-2015-594. I have just completed the uploading the reply to both Dr. Fuelistaler and an anonymous reviewer intending for the publication of final author comments through Copernicus web site.

Here I am attaching the differential file, which I prepared by using latexdiff as instructed in the mail from Copernicus, although it will be of limited use because of errors. Then I am attaching hand-made version of the differential hoping to help you check the revision.

I am also aware I need to submit revised figures. Could you instruct me how to proceed? I am willing to follow your instructions also on the English edition as commented by Dr. Fueglistaler.

I should appreciate it very much if you could find the manuscript suitable for publication in ACP as soon as possible. Thank you very much in advance.

Best regards,

Fumio Hasebe

Reply to Dr. S. Fueglistaler (referee)

We are grateful to the thorough reading and constructive comments on our manuscript. We have made substantial changes to the manuscript in response to the review as described below. Each panel of figures are labeled "a", "b" and so on as suggested, and the following reply refers to these labels. These revisions have significantly improved the manuscript, and we hope we have answered all of the concerns. We think all these improvements will satisfy the reviewer and hopefully make the manuscript suitable for publication in ACP.

Major issues

1. **Comment:** Hasebe and Noguchi present an analysis of the evolution of stratospheric water from the late 1990's to the early 2000's, where water entering the stratosphere experienced a remarkable, sudden drop in the year 2000. They use kinematic trajectory calculations based on ECMWF ERA-Interim reanalysis data, where the dehydration along the trajectories is estimated based on the temperature evolution (i.e. one assumes complete dehydration down to the minimum saturation mixing ratio encounted during ascent from the troposphere to the stratosphere). The method is similar to that in previous studies that have shown that this model calculation provides a reasonable reproduction of observed variations in water entering the stratosphere - with some caveats concerning the drop in the year 2000 (see discussion in Fueglistaler et al. 2013). Before I go into the details, I would suggest that for a revised version, the paper should be edited by a native English speaker (or perhaps ACP provides this service) - I ignore these problems here in my review. My main difficulty with the paper is that one of the key steps in the paper - the attribution of processes leading to the decrease in water vapor - is not clearly explained. If my understanding of the procedure (outlined below) is correct, I would have some serious concerns. Also, the discussion of the Sea Surface Temperature (SST) changes is very qualitative, and could be considerably shortened.

   (a) **Comment:** Should be edited by a native English speaker.

   Reply: We are sorry to have caused problem in reading the manuscript. As is mentioned, perhaps ACP provides the service. We will follow the instruction by the editor and editorial office on English editing.

   (b) **Comment:** The attribution of processes leading to the decrease in water vapor is not clearly explained.

   Reply: Revisions are made as can be seen from the reply to **Comment 2** below.

   (c) **Comment:** The discussion of the SST changes is very qualitative and could be considerably shortened.

   Reply: The paragraph discussing the SST changes has been slightly shortened. However, some more descriptions have been made to follow the comments from another reviewer. Figure 10 has been rewritten to clarify the features we see from the SST variations.

2. **Comment:** My difficulties in understanding the method refer to Sections 3.4/3.5, and Figures 5–7, and 12. It is tempting to decompose the average entry mixing ratio into the sum of contributions from different locations, with sum[f(lon,lat,time) * smr(lon,lat,time)] = H2Oentry(time), with the normalization of frequency sum[f(..)] = 1. By comparison of the map of "f" and "smr" between 2 times (say, before and after the drop), one hopes to decompose the change in H2Oentry(time1) - H2Oentry(time2) as a result of a change in the spatial distribution ("f"), and temperature (equivalent to "smr"; ignoring pressure variations). Although not formulated in this way, this is my understanding of what the authors do in Sections 3.4 and 3.5; and accompanying figures 5, 6, 7, and later 12.

   (a) **Comment:** The method to decompose the average entry mixing ratio into the sum of contribution from different location is difficult to understand.

   Reply: The following description has been added in Section 3 of the revised manuscript.

   - **Page 28043, line 13, top**: The calculations are made on a monthly basis using the three initialization days (5th, 15th and 25th of each month) at a time. The following description refers to a specific month omitting the suffix for time. Let start by assuming that the minimum saturation mixing ratio along i-th TST

trajectory ($i = 1, \cdots, N_{\rm TST}$) is denoted by $\mathrm{SMR}_{\mathrm{min}i}$. The entry value of water to the stratosphere $[\mathrm{H_2O}]_{\rm e}$ is defined as the ensemble mean value of $\mathrm{SMR}_{\rm min}$ as in Fueglistaler et al. (2005):

$$[\mathrm{H_2O}]_{\rm e} = \frac{1}{N_{\rm TST}} \sum_{i}^{N_{\rm TST}} \mathrm{SMR}_{\mathrm{min}i}. \tag{1}$$

- **Page 28045, line 7**, after "TST trajectories.": Let assume that i-th TST trajectory ($i = 1, \cdots, N_{\rm TST}$) takes minimum saturation mixing ratio ($\mathrm{SMR}_{\mathrm{min}i}$) at bin j ($j = 1, \cdots, M$), that is, the Lagrangian cold point (LCP) for i-th TST trajectory is found at bin j. If we denote the number of LCP events at bin j as $N(\mathrm{LCP} \in j)$,

$$N_{\rm TST} = \sum_{j}^{M} N(\mathrm{LCP} \in j). \tag{2}$$

Because some trajectories do not satisfy the TST condition in general, $N_{\rm TST} \leq N$, where N is the total number of initialization points used for the calculation. The probability of LCP events at bin j, $P(\mathrm{LCP} \in j)$, is defined by

$$P(\mathrm{LCP} \in j) = \frac{N(\mathrm{LCP} \in j)}{N_{\rm TST}}, \tag{3}$$

so that the normalization condition $\sum_{j}^{M} P(\mathrm{LCP} \in j) = 1$ holds.

- **Page 28045, lines 7 to 10**: The top two panels of Fig. 5 show ... posterior to the drop).

has been changed to

The top two panels of Fig. 5 show the horizontal distributions of $P(\mathrm{LCP} \in j)$ thus defined for those trajectories initialized in September 1998 and 1999 (a; prior to the drop) and September 2000, 2001 and 2002 (b; posterior to the drop). Because $N_{\rm TST}$ is different among individual September, $N_{\rm TST}$ for each month has been used as a weight in taking the averages. In other words, the calculations are made by combining the trajectories of two or three prior- or posterior-months together for the illustrations. To be more specific, the TST trajectories of September 1998 and 1999, selected from $N = 2952 \times 3 \times 2$ trajectories, are combined together for the illustration of Fig. 5(a), while those of September 2000, 2001, and 2002, selected from $N = 2952 \times 3 \times 3$ trajectories, are used for Fig. 5(b).

- **Page 28046, lines 1 to 3**: Figure 6 is the same as Fig. 5 ... rather than the probability of LCP events.

has been changed to

The ensemble mean value of $\mathrm{SMR}_{\rm min}$ at bin j, $\mathrm{SMR}(\mathrm{LCP}\in j)$, is defined by

$$\mathrm{SMR}(\mathrm{LCP} \in j) = \frac{1}{N(\mathrm{LCP} \in j)} \sum_{i}^{\mathrm{LCP}\in j} \mathrm{SMR}_{\mathrm{min}i}, \tag{4}$$

where $\sum_{i}^{\mathrm{LCP}\in j}$ indicates the sum with respect to the subset of TST trajectories that take LCP at bin j.
Figure 6 is the same as Fig. 5 except that $\mathrm{SMR}(\mathrm{LCP}\in j)$ is illustrated rather than $P(\mathrm{LCP} \in j)$.

- **Page 28046, lines 16 to 20**: the comparisons based only on the changes ...

$\mathrm{SMR}_{\mathrm{min}}$ (Fig. 6) together for each bin.

has been changed to

the comparisons based only on the changes in SMR(LCP$\in j$) could be misleading, because the values of $P(\mathrm{LCP} \in j)$ are much higher in the former than in the latter (Fig. 5). The expectation value for bin j, $E(\mathrm{LCP} \in j)$, is defined by the multiple of $P(\mathrm{LCP} \in j)$ and SMR(LCP$\in j$) to quantify the contribution of each bin to $[\mathrm{H_2O}]_{\mathrm{e}}$. The sum of $E(\mathrm{LCP} \in j)$ with respect to all bins reduces to

$$\sum_{j}^{M} E(\mathrm{LCP} \in j) = \sum_{j}^{M} P(\mathrm{LCP} \in j) \times \mathrm{SMR}(\mathrm{LCP} \in j) \quad (5)$$

$$= \sum_{j}^{M} \frac{N(\mathrm{LCP} \in j)}{N_{\mathrm{TST}}} \times \frac{1}{N(\mathrm{LCP} \in j)} \sum_{i}^{\mathrm{LCP} \in j} \mathrm{SMR}_{\mathrm{min}i} \quad (6)$$

$$= \frac{1}{N_{\mathrm{TST}}} \sum_{j}^{M} \sum_{i}^{\mathrm{LCP} \in j} \mathrm{SMR}_{\mathrm{min}i} \quad (7)$$

$$= \frac{1}{N_{\mathrm{TST}}} \sum_{i}^{N_{\mathrm{TST}}} \mathrm{SMR}_{\mathrm{min}i}. \quad (8)$$

This is the entry value of water to the stratosphere $[\mathrm{H_2O}]_{\mathrm{e}}$ (Eq. (1)) shown as a time series in Fig. 3. $[\mathrm{H_2O}]_{\mathrm{e}}$ is thus decomposed of the sum of $E(\mathrm{LCP} \in j)$, which is interpreted as the contribution of bin j to $[\mathrm{H_2O}]_{\mathrm{e}}$. What is important here is that it is neither $P(\mathrm{LCP} \in j)$ nor SMR(LCP$\in j$) but the product between the two, $E(\mathrm{LCP} \in j)$, that is directly responsible for composing the value $[\mathrm{H_2O}]_{\mathrm{e}}$. By comparing the distribution of $E(\mathrm{LCP} \in j)$ between the two periods, prior and posterior to the drop, we can see how the drop in $[\mathrm{H_2O}]_{\mathrm{e}}$ is brought about by the change of water transport from individual region.
Figure 7 shows the horizontal distribution of $E(\mathrm{LCP} \in j)$.

(b) **Comment:** Figures 5, 6, 7 and 12 are difficult to understand.

Reply: The top two panels of Figs. 5 and 6 show the spatial distributions of $P(\mathrm{LCP} \in j)$ and SMR(LCP$\in j$), respectively, for September, and those of Figs. 7 and 12 are the spatial distributions of $E(\mathrm{LCP} \in j)$ for September and January, respectively. The September (January in Fig. 12) values prior and posterior to the drop are estimated by averaging two or three years of the corresponding month. Because N_{TST} is different among individual September, N_{TST} for each month has been used as a weight in taking the averages. In other words, the calculations written above are made by combining two or three prior- or posterior-months together for the illustrations of these figures. To be more specific, the TST trajectories of September 1998 and 1999, selected from $N = 2952 \times 3 \times 2$ trajectories, are combined together for the illustration of the panel (a) of Figs. 5, 6, and 7, while those of September 2000, 2001, and 2002, selected from $N = 2952 \times 3 \times 3$ trajectories, are used for the illustration of panel (b) of these figures. These explanations are supplemented in Section 3.1 as described above.

3. **Comment:** Figure 5 then shows a shift in the locations where the last dehydration occurs, and Figure 6 then shows a change in temperatures. What is then observed is that some regions cool more than others, and that in these regions the fraction of "Lagrangian cold points" (LCP) increases. In other words, the LCP distribution is highly correlated with the distribution of the difference in temperature relative to the tropical mean. (As demonstrated in Fueglistaler and Haynes, 2005; their figure 2c, d).

Reply: The LCP distribution may appear "highly correlated with the distribution of the difference relative to the tropical mean." However, closer look will find that high values of $P(\mathrm{LCP} \in j)$ are concentrated in the region over the Bay of Bengal and Malay Peninsula in September (Fig. 5), while low values of SMR(LCP$\in j$) are found widely distributed in the western tropical Pacific (Fig. 6). The novelty of our analysis is to have distinguished the distribution of $P(\mathrm{LCP} \in j)$

against SMR(LCP$\in j$) and introduced $E(\text{LCP} \in j)$. Please see the Reply to **Comment 4** below.

4. **Comment:** The problem then is the interpretation.

   (a) **Comment:** The high correlation of the perturbations in the spatial distribution of the LCP density, and temperature (i.e. the cross term f-prime × smr-prime) prevents an interpretation in terms of "contribution from spatial change in LCP density". Very problematic are statements like (Page 28046/Line 24): "The reductions (bottom panel) are mainly due to the decreases of the LCP-event probability ..." One cannot say that because some region now has a lower frequency, that this contributes to a lower average H2O entry - if only says that fewer air parcels are last dehydrated there (i.e. the term "f-prime × smr-mean" can only be interpreted for the total domain sum, not for individual regions!) But perhaps I simply don't quite understand what exactly you show in Figure 7 - you need to provide an equation to explain properly what exactly you calculate.

   Reply: We hope the equations (1) through (8) above, being added in the revised manuscript, have made the quantity shown in Fig. 7 clear. We can interpret the values of $E(\text{LCP} \in j)$ as the contribution of bin j to $[\text{H}_2\text{O}]_\text{e}$. As the quantity that directly drives $[\text{H}_2\text{O}]_\text{e}$ is $E(\text{LCP} \in j)$, any statement that attributes solely $P(\text{LCP} \in j)$ or SMR(LCP$\in j$) to the cause of changes in $[\text{H}_2\text{O}]_\text{e}$ is mathematically wrong. However, we believe it is quite interesting to see individual changes in $P(\text{LCP} \in j)$ and SMR(LCP$\in j$) to interpret the variations in $E(\text{LCP} \in j)$. The paragraph that includes the "very problematic" sentence is a part of our effort along this line, trying to interpret the noticeable features in $E(\text{LCP} \in j)$ as meteorological words with the hope to help understand the changes in terms of modulated trajectories and perturbed temperature. The cited sentence and the one that follows are replaced by the following in the revised manuscript.

   - **Page 28046, line 23 to page 28047, line 1**: The contribution from this core area ... decrease in SMR_min.

   has been changed to

   The contribution from this core area remains dominant during the posterior period (Fig. 7(b)). While the reduction of $[\text{H}_2\text{O}]_\text{e}$ cannot be free from the general cooling (lowering of SMR(LCP$\in j$)) in posterior years over most of the tropics (Fig. 6), it is interesting to note the increase of $E(\text{LCP} \in j)$ despite the decrease in SMR(LCP$\in j$) over the central Pacific. This is because the increase of $P(\text{LCP} \in j)$ more than compensate for the decrease of SMR(LCP$\in j$) over there. In this sense, it is not appropriate to attribute the cooling over the western and the central Pacific to the drop in $[\text{H}_2\text{O}]_\text{e}$. The similarity in the spatial distributions of $P(\text{LCP} \in j)$ and $E(\text{LCP} \in j)$, especially that of the location of maxima over the Bay of Bengal and Malay Peninsula together with the post 2000 decrease over there and the western tropical Pacific, suggests that the relocation of LCPs (change in $P(\text{LCP} \in j)$) is a leading factor that has caused the drop in $[\text{H}_2\text{O}]_\text{e}$ in September 2000.

   (b) **Comment:** To make my point clearer, consider the following case: The temperature field is homogenous (i.e. constant) at the tropical tropopause with a just a little bit of noise. The resulting LCP distribution would be pretty much random, but because of finite sampling, there would be some regions where there would be a bit higher densities, and some regions with lower densities. Now we do the experiment a second time, and look at the differences in the LCP distribution. We would see some regions with a decrease, and some regions with an increase in density. Now, the regions where the density decreases (i.e. "f-prime" would be negative) now seem to contribute to a "drying" if we quantify the contributions to the average H2Oentry as being the product of smr and density. However, since the locations simply have shifted in space and no real temperature change has taken place, we would observe similarly regions that seem to have contributed to a "moistening" simply because "f-prime" in these regions is positive. Of course, the "moistening" would simply balance the "drying" elsewhere, and the net change in H2Oentry is zero. Hence, this method produces spurious results.

   Reply: The statistical significance is always an issue to be payed attention to. We cannot conclude anything from the example indicated above. By employing large number of trajectories, however, we believe we have attained the statistical significance high enough to

derive meaningful results. The statistical significance of the estimated differences between the two periods in $P(\mathrm{LCP} \in j)$ and $\mathrm{SMR}(\mathrm{LCP} \in j)$ are shown at the bottom panels (d) of Figs. 5 and 6. Our argument in the manuscript is concerned only with those regions we confirmed the statistical significance is high. The following revision has been made.

- **Page 28041, lines 5 to 13**: The trajectory calculations are started from uniformly distributed gridpoints ... horizontal resolution of 0.75° by 0.75° longitude–latitude gridpoints prior to calculations.

has been changed to

The backward trajectory calculations are started from uniformly distributed gridpoints (every 5.0° longitude by 1.5° latitude) within 30° N and S from the equator on 400 K potential temperature surface. The initializations are made on the 5th, 15th, and 25th of every month during the period since January 1997 till December 2002 relying on the European Centre For Medium-Range Weather Forecasts ERA Interim dataset (Dee et al., 2011). The number of initialization points is 2952 for a single calculation resulting in 8856 for the estimation of monthly values. This number compares well with that of the reduced set of trajectories in the study on the sensitivity of number of trajectories by Bonazzola and Haynes (2004) and turned out to be enough to derive statistically significant results as can be seen later in Section 3. All meteorological variables given on 60 model levels have been interpolated to those on 91 pressure levels keeping the horizontal resolution of 0.75° by 0.75° longitude-latitude gridpoints prior to calculations. The time step has been set to 30 minutes, similar to 36 minutes taken by Bonazzola and Haynes (2004), by applying spatiotemporal interpolations to the 6-hour interval ERA Interim dataset. As for the limitation and caution of this method, see, for example, the pioneering studies by Fueglistaler et al. (2004) and Bonazzola and Haynes (2004).

Some further comments

1. **Comment:** P28038/L3: "... after a prolonged increase through the 1980's and 1990's." I'd formulate this a bit more careful.

   Reply: The sentence has been revised as follows:

   - **Page 28038, lines 2 to 3**: Stratospheric water vapor is known to have decreased suddenly at around the year 2000 to 2001 after a prolonged increase through the 1980s and 1990s.

   has been changed to

   The sudden decrease of stratospheric water vapor at around the year 2000 to 2001 is relatively well accepted in spite of the difficulty to quantify the long-term variations.

2. **Comment:** P28047/L16: I would think that Figure 2B of Fueglistaler and Haynes (2005) pretty convincingly shows that indeed the high values in the first half of 1998 are due to ENSO.

   Reply: The following sentence has been inserted after "in these months."

   - **Page 28047, line 16**: Actually Fueglistaler and Haynes (2005) demonstrated in their Fig. 2 that the trajectory model shows large increase of lower-stratospheric water ($[\mathrm{H_2O}]_{\mathrm{T400}}$ which takes non-TST trajectories into account in addition to $[\mathrm{H_2O}]_{\mathrm{e}}$) associated with El Niño and that the increase is accompanied by the eastward shift of the high density region of LCP.

3. **Comment:** P28048/L16ff: Figure 4 and the discussion here is not convincing; surely panels (a) and (b) look somewhat different but it's impossible to say anything quantitative. I suggest to eliminate this figure.

   Reply: It is true that Figure 4 cannot show any quantitative change in the LCP distribution; such a role is assigned to Figure 5. The purpose of Figure 4 is to get a clear view on how the TTL trajectories in August are distributed. This is a basic information to proceed to the interpretation of the results shown later, and thus Figure 4 is retained.

4. **Comment:** P28048/L1ff: Figure 9 is very nice! I wonder whether this figure should not be presented before the "Lagrangian Figures 6, 7, 8", since this Eulerian perspective really helps to understand what happens in the Lagrangian perspective.

   Reply: Our main purpose is to examine the change of $[H_2O]_e$ from a Lagrangian perspective and try to interpret it from a meteorological point of view. Figure 9, together with Figure 4, is quite impressive and suggests the direction of further research. However, it does not necessarily mean Figure 9 is better presented earlier than Figures 6, 7, and 8. The sequence of figures is kept intact.

5. **Comment:** P28049/L8ff: You state that post-2000 there was a "loosened grip" of the Tibetan high on air parcels - are you sure that this is the main reason for the shift in the spatial distribution of the LCPs? Alternative explanations: (i) Even with identical path, the post-2000 temperature pattern would induce a shift in the LCP distribution simply because the probability to encounter minimum temperatures has increased over the tropical Western Pacific region; and (ii) the temperature pattern change came about by a shift in deep convection, with more convection over the tropical Western Pacific, and the air masses reaching the TTL in that convection may never be part of the Tibetan anticyclone.

   Reply: The description "loosened grip" comes from our speculation based on the changes in the TTL trajectories shown in Figure 4 combined with the weakened Tibetan high in the posterior years seen from Figure 9. The alternative explanation (i) will not apply because we can see from Figs. 4 and 5 that the density of trajectories circulating Tibetan high is substantially lower while more trajectories are found in the southern hemisphere in the posterior years. The alternative explanation (ii) is interesting in that the trajectories do change even if there is no modulation in Tibetan high. However, we do not adopt this interpretation since we do see weakening of Tibetan high in posterior years. In our opinion, the speculative expression "loosened grip" is acceptable in discussion section.

6. **Comment:** P28049/L18ff/Figure 10: I am not convinced by what I see in this Figure, nor by your description. What is visible are variations due to ENSO - I would argue no neutral person not knowing about the drop in the year 2000 would see anything special around the year 2000 in this figure.

   Reply: Figure 10 has been rewritten to shed light on the eastward migration of 28°C SST contour. The reason why we pay attention to this contour is based on the paper by Gadgil et al. (1984), who pointed out that 28°C is a threshold of active convection (page 28049, line 22).

7. **Comment:** P28051/L4ff: This is an interesting hypothesis! My only concern is that in our studies we operated with monthly means, and I would be cautious about the significance of a 1-month difference.

   Reply: The September values of $[H_2O]_e$ are calculated using the trajectories initialized on 5th, 15th and 25th of September. The backward 90-day trajectory calculations rely on the meteorological fields in August, July and June; there is no reference to October values. In this sense, the one month difference is significant.

8. **Comment:** P28051/L22/Figure 12: As said for Figure 7, I need to see an equation to fully understand what this figure shows.

   Reply: Done.

9. **Comment:** P28052/L3ff: "These evidences ..." I could not follow your arguments here. The eastward expansion of warm water should lead to a cooling over these regions, but in Figure 12, the "difference" shown in the bottom panel is "red" over the central Pacific, while it is blue over the Maritime continent - supposedly to the *WEST* of the convection anomaly? Please clarify.

   Reply: Your expectation concerns the change in SMR(LCP$\in j$) while the above sentence deals with $E(\text{LCP} \in j)$. The decrease in SMR(LCP$\in j$) is more than compensated by the increase in $P(\text{LCP} \in j)$, resulting in the increase in $E(\text{LCP} \in j)$ in the central Pacific (red). Related sentences are revised as follows:

- **Page 28051, line 27 to page 28052, line 5**: The difference between the two periods ... the central Pacific (Fig. 10).

has been changed to

The difference between the two periods (Fig. 12(c)) shows decrease over Indonesia and increase over the central Pacific during the period posterior to the drop. The former is due to the combination of the decreases in both $P(\mathrm{LCP} \in j)$ and $\mathrm{SMR}(\mathrm{LCP} \in j)$, while the latter is brought about by the interplay between the increase in $P(\mathrm{LCP} \in j)$ and some decrease of $\mathrm{SMR}(\mathrm{LCP} \in j)$ (not shown). This situation is the same as what we see in September (Section 3.5). The similarity of this pattern, that is, the decrease in the equatorial western Pacific (over Indonesia) and the increase over the central Pacific, to that of the second component of September response suggests the existence of a common driver of the drop in $[\mathrm{H_2O}]_\mathrm{e}$ irrespective of the season. These evidences suggest the idea that the drop of $[\mathrm{H_2O}]_\mathrm{e}$ in northern winter has resulted from the response of the TTL circulation to the eastward expansion of the warm water to the central Pacific (Fig. 10) in such a way that the decrease of $E(\mathrm{LCP} \in j)$ in the western Pacific exceeds the increase of that in the central Pacific.

10. **Comment:** Figures: Please add labels ("a", "b" etc) to all sub-plots.

    Reply: Done.

11. **Comment:** Figure 3: I understand that you are concerned that a 6-year period is too short to define a reliable climatology, but I would still consider a decomposition into mean annual cycle, and anomalies thereof, to be the better solution. Since you use the same method and data as Fueglistaler et al. (2013), you could check whether your anomalies look similar to those that they published (e.g. their Figure 8b) to make sure that the comparatively short timescale does not distort the anomalies too much.

    Reply: I understand the time series labeled by EI in Figure 8(b) of Fueglistaler et al. (2013) is the anomalies from the mean of more than 20 years from 1989 to 2011. The anomalies of our 6-year time series is not suitable for comparison because of the large influence of 1997-1998 El Niño. This is what we found at the earliest stage of our analysis.

12. **Comment:** Figure 6: Please change the color scale of panel "c" to the same as in Figure 5 (i.e. going from blue to red with white at 0).

    Reply: Done.

13. **Comment:** Figure 7: As mentioned before, please provide an equation for what is shown in this figure, and improve the figure caption.

    Reply: The equations are provided in response to **Comment 2** of Major issues. The figure caption has been changed to the following.

    - **Figure 7**. The same as the top three panels of Fig. 6 except that $E(\mathrm{LCP} \in j)$, the contribution of bin j to $[\mathrm{H_2O}]_\mathrm{e}$, (ppmv) is illustrated. See text for the definition of $E(\mathrm{LCP} \in j)$.

Reply to Anonymous Referee #1

We thank the thorough reading and constructive comments on our manuscript. We have made substantial changes to the manuscript in response to the review as described below. Each panel of figures are labeled "a", "b", "c" and "d" from the top to the bottom if exists, and the following reply refers to these labels. These revisions have significantly improved the manuscript, and we hope we have answered all of the concerns. We think all these improvements will satisfy the reviewer and hopefully make the manuscript suitable for publication in ACP.

General comments

1. **Comment:** This manuscript describes the change of pathways of backward kinematic trajectories initialized at 400 K height level from a period before and after the stratospheric water vapour (SWV) drop in the year 2000. The authors discuss the cause of the stepwise drop in SWV by an analysis of the water vapour entry values to the stratosphere. They focus on the month of September in the period 1998-2002, because the drop in H2O entry values first occurred at that month. The authors' conclusions are that the low H2O entry values to the stratosphere in September 2000 and the sustained low values thereafter can be interpreted as being driven by changes in thermal forcing from the earth's surface.

   I recommend major revisions before a potential publication of the manuscript in ACP.

   Reply: We have made substantial changes to the manuscript in response to the review as described below, and we hope we have answered all of the concerns raised by the reviewer.

Specific comments

1. **Comment:** Two former publications of 1. by Bonazzola and Haynes (2004), who performed a trajectory analysis on the basis of ECMWF operational analysis data for the period prior to the drop (1997-1999) and 2. by Fueglistaler, Wernli and Peter (2004), who analysed the troposphere-to-stratosphere transport in the time period January/February and July/August for the year 2001 (i.e. posterior to the drop), and probably relevant to this study, are considered neither in the introduction nor in the results. The authors should compare their results with those of these older ones. In particular I would like to see what is new in the current manuscript.

   Reply: Thank you for pointing out important papers not referenced in this study. Both papers are referred to in Sections 1 and 3 of revised manuscript as the pioneering studies using the trajectories in TTL dehydration. The comparison of the results with those of former research is made, although it is not straightforward because of the differences in the analyzed quantities as well as the datasets having been used. It is well known that the entry value of water to the stratosphere $[H_2O]_e$ depends on two factors: the pathways taken by trajectories and the temperature distribution in the TTL. The former describes the efficiency of sampling the coldest region by air parcels and the latter is related with the coldest temperature irrespective of the trajectory distribution, and are called "the sampling effect" and the "temperature effect", respectively, by Bonazzola and Haynes (2004). These authors estimated the importance of both effects on the intraseasonal and interannual time scales. What is new in the present study is to have decomposed $[H_2O]_e$ into the regional contributions (Fig. 7) by estimating the frequency distribution of LCP (Fig. 5) and temperature minima ($\sim SMR_{min}$ in Fig. 6), respectively, on a regional basis, and applied it to solve the problem of the SWV drop in 2000.

   The following revisions are made in Section **1 Introduction**,

   - **Page 28039, lines 24 to 27**: The reproduction of SWV variations by using the Lagrangian temperature history along the trajectories (e.g., Fueglistaler et al., 2005; Dessler et al., 2014) has proven quite effective, even though ...

   has been changed to

   The Lagrangian description of the transport processes in the tropical troposphere to the stratosphere using trajectory calculations proved to be quite effective not only in the reproduction of SWV variations but also in the characterization of the dehydration processes in the TTL (e.g., Bonazzola and Haynes, 2004; Fueglistaler et al., 2004, 2005; Dessler et al., 2014) even though ...

and **3 Results**

- **Page 28045, lines 10 to 13**: The spatial maximum during the period ... this maximum shows eastward expansion as far as 150° E.

has been changed to

The comparison between the two will shed light on the change in "the sampling effect" of Bonazzola and Haynes (2004). The spatial distribution is characterized by the maxima over the Bay of Bengal and Malay Peninsula accompanied by a ridge extending to South China Sea. It is interesting to note some similarity in the location to the spatial maxima of the first encounter of backward trajectories to 370 K isentrope for June to August 1999 shown by Bonazzola and Haynes (2004). During the period posterior to the drop (Fig. 5(b)), the maxima show eastward expansion as far as 150°E.

- **Page 28045, line 27**: The following sentence is inserted after "the SMR_{min}."
This corresponds to focus on the change in "the temperature effect" of Bonazzola and Haynes (2004).

- **Page 28046, lines 6 to 9**: The values show general decrease ... between the two (third panel),

has been changed to

The values show general decrease in the tropics with some enhanced drop in the central Pacific reaching less than 3.0 ppmv in the period posterior to the drop (Fig. 6(b)). The gross features correspond well to the horizontal distribution of the LCP-averaged SMR of July/August 2001 estimated by Fueglistaler et al. (2004). The difference between the two periods (Fig. 6(c)),

2. **Comment:** In Section 2.1 you state that your method is similar to that of Fueglistaler et al., 2005. I suggest that you describe at least the main aspects of your method (e.g. in an Appendix), so that the reader can understand what you did without reading the afore-mentioned paper. Please provide as well more information on the calculation of the trajectories. For instance: which time interval of ERA-interim data was available for interpolation? As ERA-interim has 6 hours output interval, do you consider this sufficient for temporal interpolation? Also, how many trajectories do you analyse in total? Is this sufficient for robust results?

Reply: Spatiotemporal interpolations necessary to conduct trajectory calculations have been written in Section 2.1, while the brief description on the main aspects of the method is introduced in Section 3.1. The following revisions are made in Section **2.1 Trajectory calculations**,

- **Page 28041, lines 5 to 11**: The trajectory calculations are started from uniformly distributed gridpoints ... ERA Interim dataset (Dee et al., 2011).

has been changed to

The backward trajectory calculations are started from uniformly distributed gridpoints (every 5.0° longitude by 1.5° latitude) within 30° N and S from the equator on 400 K potential temperature surface. The initializations are made on the 5th, 15th, and 25th of every month during the period since January 1997 till December 2002 relying on the European Centre For Medium-Range Weather Forecasts ERA Interim dataset (Dee et al., 2011). The number of initialization points is 2952 for a single calculation resulting in 8856 for the estimation of monthly values. This number compares well with that of the reduced set of trajectories in the study on the sensitivity of number of trajectories by Bonazzola and Haynes (2004) and turned out to be enough to derive statistically significant results as can be seen later in Section 3.

and the following sentences are inserted in **3 Results**

- **Page 28043, line 13, top**: The calculations are made on a monthly basis using the three initialization days (5th, 15th and 25th of each month) at a time. The following description refers to a specific month omitting the suffix for time. Let start by assuming

that the minimum saturation mixing ratio along i-th TST trajectory ($i = 1, \cdots, N_{\mathrm{TST}}$) is denoted by $\mathrm{SMR}_{\mathrm{min}i}$. The entry value of water to the stratosphere $[\mathrm{H_2O}]_{\mathrm{e}}$ is defined as the ensemble mean value of $\mathrm{SMR}_{\mathrm{min}}$ as in Fueglistaler et al. (2005):

$$[\mathrm{H_2O}]_{\mathrm{e}} = \frac{1}{N_{\mathrm{TST}}} \sum_{i}^{N_{\mathrm{TST}}} \mathrm{SMR}_{\mathrm{min}i}. \tag{1}$$

- **Page 28045, line 7**, after "TST trajectories.": Let assume that i-th TST trajectory ($i = 1, \cdots, N_{\mathrm{TST}}$) takes minimum saturation mixing ratio ($\mathrm{SMR}_{\mathrm{min}i}$) at bin j ($j = 1, \cdots, M$), that is, the Lagrangian cold point (LCP) for i-th TST trajectory is found at bin j. If we denote the number of LCP events at bin j as $N(\mathrm{LCP} \in j)$,

$$N_{\mathrm{TST}} = \sum_{j}^{M} N(\mathrm{LCP} \in j). \tag{2}$$

Because some trajectories do not satisfy the TST condition in general, $N_{\mathrm{TST}} \leq N$, where N is the total number of initialization points used for the calculation. The probability of LCP events at bin j, $P(\mathrm{LCP} \in j)$, is defined by

$$P(\mathrm{LCP} \in j) = \frac{N(\mathrm{LCP} \in j)}{N_{\mathrm{TST}}}, \tag{3}$$

so that the normalization condition $\sum_{j}^{M} P(\mathrm{LCP} \in j) = 1$ holds.

- **Page 28045, lines 7 to 10**: The top two panels of Fig. 5 show ... posterior to the drop).

has been changed to

The top two panels of Fig. 5 show the horizontal distributions of $P(\mathrm{LCP} \in j)$ thus defined for those trajectories initialized in September 1998 and 1999 (a; prior to the drop) and September 2000, 2001 and 2002 (b; posterior to the drop). Because N_{TST} is different among individual September, N_{TST} for each month has been used as a weight in taking the averages. In other words, the calculations are made by combining the trajectories of two or three prior- or posterior-months together for the illustrations. To be more specific, the TST trajectories of September 1998 and 1999, selected from $N = 2952 \times 3 \times 2$ trajectories, are combined together for the illustration of Fig. 5(a), while those of September 2000, 2001, and 2002, selected from $N = 2952 \times 3 \times 3$ trajectories, are used for panel Fig. 5(b).

- **Page 28046, lines 1 to 3**: Figure 6 is the same as Fig. 5 ... rather than the probability of LCP events.

has been changed to

The ensemble mean value of $\mathrm{SMR}_{\mathrm{min}}$ at bin j, $\mathrm{SMR}(\mathrm{LCP} \in j)$, is defined by

$$\mathrm{SMR}(\mathrm{LCP} \in j) = \frac{1}{N(\mathrm{LCP} \in j)} \sum_{i}^{\mathrm{LCP} \in j} \mathrm{SMR}_{\mathrm{min}i}, \tag{4}$$

where $\sum_{i}^{\mathrm{LCP} \in j}$ indicates the sum with respect to the subset of TST trajectories that take LCP at bin j.
Figure 6 is the same as Fig. 5 except that $\mathrm{SMR}(\mathrm{LCP} \in j)$ is illustrated rather than $P(\mathrm{LCP} \in j)$.

- **Page 28046, lines 16 to 20**: the comparisons based only on the changes ... $\mathrm{SMR}_{\mathrm{min}}$

(Fig. 6) together for each bin.

has been changed to

the comparisons based only on the changes in SMR(LCP$\in$ j) could be misleading, because the values of P(LCP $\in$ j) are much higher in the former than in the latter (Fig. 5). The expectation value for bin j, E(LCP $\in$ j), is defined by the multiple of P(LCP $\in$ j) and SMR(LCP$\in$ j) to quantify the contribution of each bin to $[H_2O]_e$. The sum of E(LCP $\in$ j) with respect to all bins reduces to

$$\sum_j^M E(\mathrm{LCP} \in j) = \sum_j^M P(\mathrm{LCP} \in j) \times \mathrm{SMR}(\mathrm{LCP} \in j) \quad (5)$$

$$= \sum_j^M \frac{N(\mathrm{LCP} \in j)}{N_{\mathrm{TST}}} \times \frac{1}{N(\mathrm{LCP} \in j)} \sum_i^{\mathrm{LCP} \in j} \mathrm{SMR}_{\mathrm{min}i} \quad (6)$$

$$= \frac{1}{N_{\mathrm{TST}}} \sum_j^M \sum_i^{\mathrm{LCP} \in j} \mathrm{SMR}_{\mathrm{min}i} \quad (7)$$

$$= \frac{1}{N_{\mathrm{TST}}} \sum_i^{N_{\mathrm{TST}}} \mathrm{SMR}_{\mathrm{min}i}. \quad (8)$$

This is the entry value of water to the stratosphere $[H_2O]_e$ (Eq. (1)) shown as a time series in Fig. 3. $[H_2O]_e$ is thus decomposed of the sum of E(LCP $\in$ j), which is interpreted as the contribution of bin j to $[H_2O]_e$. What is important here is that it is neither P(LCP $\in$ j) nor SMR(LCP$\in$ j) but the product between the two, E(LCP $\in$ j), that is directly responsible for composing the value $[H_2O]_e$. By comparing the distribution of E(LCP $\in$ j) between the two periods, prior and posterior to the drop, we can see how the drop in $[H_2O]_e$ is brought about by the change of water transport from individual region.
Figure 7 shows the horizontal distribution of E(LCP $\in$ j).

3. **Comment:** In sections 3.4/3.5 you show that the horizontal distribution of LCP-event probability (Fig. 5) shifts from Bay of Bengal and the Western Pacific area to the Central Pacific. Fig. 7 shows that the contribution of the region from which the water vapour enters the stratosphere shifts in the same way. However, this effect is accompanied by a general decrease in H2O entry values over most of the tropical area (Fig. 6(b)) and a strong temperature decrease at 100 hPa (Fig. 9), which is most prominent in the Central Pacific. I wonder whether it is not this cooling at 100 hPa which is the dominant process for the water vapour drop instead of the shift of trajectories entering the stratosphere. Thus I would like to see more evidence for your suggestion that it is the shift of the trajectories rather than the strong cooling at 100 hPa that leads to the water vapour drop. My feeling is that it is not possible to disentangle these two influences with your analysis.

   Reply: Thank you pointing out the important issue to be explained in more detail. As is shown by Eq. (8), we can interpret the values of E(LCP $\in$ j) as the contribution of bin j to $[H_2O]_e$. Because the quantity that directly drives $[H_2O]_e$ is E(LCP $\in$ j), any statement that attributes solely P(LCP $\in$ j) or SMR(LCP$\in$ j) to the cause of changes in $[H_2O]_e$ is mathematically wrong. However, we believe it is quite interesting to see individual changes in P(LCP $\in$ j) and SMR(LCP$\in$ j) to interpret the variations in E(LCP $\in$ j). The following revision is made in the revised manuscript.

   - **Page 28046, line 23 to page 28047, line 1**: The contribution from this core area ... decrease in $\mathrm{SMR}_{\mathrm{min}}$.

   has been changed to

   The contribution from this core area remains dominant during the posterior period (Fig. 7(b)). While the reduction of $[H_2O]_e$ cannot be free from the general cooling (lowering of SMR(LCP$\in$ j)) in posterior years over most of the tropics (Fig. 6), it is interesting to note the increase of E(LCP $\in$ j) despite the decrease in SMR(LCP$\in$ j)

over the central Pacific. This is because the increase of $P(\mathrm{LCP} \in j)$ more than compensate for the decrease of $\mathrm{SMR}(\mathrm{LCP} \in j)$ over there. In this sense, it is not appropriate to attribute the cooling over the western and the central Pacific to the drop in $[\mathrm{H_2O}]_\mathrm{e}$. The similarity in the spatial distributions of $P(\mathrm{LCP} \in j)$ and $E(\mathrm{LCP} \in j)$, especially that of the location of maxima over the Bay of Bengal and Malay Peninsula together with the post 2000 decrease over there and the western tropical Pacific, suggests that the relocation of LCPs (change in $P(\mathrm{LCP} \in j)$) is a leading factor that has caused the drop in $[\mathrm{H_2O}]_\mathrm{e}$ in September 2000.

4. **Comment:** Page: 28040, line 10: What do you mean by occasional value?

   Reply: "its occasional value ($\mathrm{SMR_{min}}$)" has been changed to "the minimum value ($\mathrm{SMR_{min}}$)".

   Comment: line 20: however, it will... What is meant by "it"?

   Reply: The sentence has been changed to

   However, such a restriction will serve to focus our investigation on some specific processes that may have led to ...

   Comment: line 21: "the advantages". Please specify the advantages or omit the "the".

   Reply: "the advantages" has been replaced by "an advantage".

5. **Comment:** Page 28041, line 12: What is meant by "those on pressure levels"? Which variables are on pressure levels?

   Reply: The sentence has been replaced by

   - **Page 28041, line 11ff**: All meteorological variables given on 60 model levels have been interpolated to those on 91 pressure levels keeping the horizontal resolution of 0.75° by 0.75° longitude-latitude gridpoints prior to calculations. The time step has been set to 30 minutes, similar to 36 minutes taken by Bonazzola and Haynes (2004), by applying spatiotemporal interpolations to the 6-hour interval ERA Interim dataset. As for the limitation and caution of this method, see, for example, the pioneering studies by Fueglistaler et al. (2004) and Bonazzola and Haynes (2004).

6. **Comment:** Page 28042, line 19: If you use ERA-interim data for the calculation of backward trajectories, how is a time step of 30 minutes possible? Please provide some information why 0.2 K in potential temperature within one time step defines a fast ascending air parcel.

   Reply: The ERA Interim gridpoint values in the time interval of 6 hours are interpolated in both time and space to the location of air parcels every time step of trajectory calculation as is described above. The increment of 0.2 K has been chosen empirically. The following revision is made.

   - **Page 28042, line 18**: The required rate for the fast ascent is empirically set to more than 0.2 K in potential temperature within 1 time step (30 min),

   Comment: line 24: "rapidly decays" is probably the wrong expression. Do you mean the proportion of fast air parcel go to zero?

   Reply: "rapidly decays" has been replaced by "rapidly goes to near zero".

7. **Comment:** Page 28045, line 2: The reference to figure 4 of Randel and Jensen is misleading. It shows the intrusion of ozone-rich air, which I expect to be of stratospheric origin and thus dry air.

   Reply: As the influence from the extratropics is out of the scope of the present study, the sentence is deleted. The related changes are

   - **Page 28044, line 24 to page 28045, line 4**: dehydration efficiency in the TTL. ... associated with the modal shift seen in Fig. 4,

   has been changed to

   dehydration efficiency in the TTL. To quantify the change in the LCP distribution associated with the modal shift seen in Fig. 4,

8. **Comment:** Page 28046, line 10: Please provide information about the statistics ("significance") including the respective formulas you used. I do not understand how the t-test is applied for your samples. I expect to see arguments why you think your applied statistics method is suitable. You might do this in an appendix.

Reply: The method of estimating the statistical significance has been written in Appendix, which will read as follows:

Appendix A: Statistical tests between prior and posterior to the drop

A1 The difference of $P(\text{LCP} \in j)$

Let the random variable, X, is the number of event occurrences in some number of trials, n. The binomial distribution can be used to calculate the probabilities for each of $n+1$ possible values of X $(X = 0, 1, \cdots, n)$ if the following conditions are met: (1) the probability of the event occurring does not change from trial to trial, and (2) the outcomes on each of the n trials are mutually independent. These conditions are rarely met, but real situations can be close enough to this ideal that the binomial distribution provides sufficiently accurate representations. The probability that the number of occurrence X is x among n trials, $\Pr(X = x)$, follows the binomial distribution

$$\Pr(X = x) = \left(\begin{array}{c} n \\ x \end{array} \right) p^x (1-p)^{n-x}, \quad (x = 0, 1, \cdots, n), \tag{9}$$

where p is the probability of occurrence of the event.

The statistical test for the difference in the population proportion of two binomial populations, $p_1 - p_2$, could be made as follows. Let the sample size and the sample proportion of the two sets being n_1 and n_2 and m_1/n_1 and m_2/n_2, respectively. The test statistic, T_1, defined by

$$T_1 = \frac{m_1/n_1 - m_2/n_2}{\sqrt{p^*(1-p^*)(1/n_1 + 1/n_2)}}, \quad p^* = \frac{m_1 + m_2}{n_1 + n_2}, \tag{10}$$

follows approximately the standard normal distribution. The statistical test for the difference between $P(\text{LCP} \in j)$ in prior and posterior periods could be done by applying the two-sided tests under the null hypothesis of $p_1 - p_2 = 0$ at some significance level α, where p_1 and p_2 are the population proportion of LCP taking place at bin j in the posterior and prior to the drop, respectively. In our case, n_1 and n_2, and m_1 and m_2, are N_{TST} and $N(\text{LCP} \in j)$, respectively, for posterior (suffix 1) and prior (suffix 2) periods.

A2 The difference of $\text{SMR}(\text{LCP} \in j)$

The statistical test to be applied is the comparison of the population means of two normal distributions, μ_1 and μ_2, with unknown population variances. This test is sometimes called the Welch's t test. The test statistic, T_2, defined by

$$T_2 = \frac{\overline{x}_1 - \overline{x}_2}{\sqrt{s_1^2/n_1 + s_2^2/n_2}}, \tag{11}$$

follows the t distribution of the degree of freedom m, where

$$m = \frac{(s_1^2/n_1 + s_2^2/n_2)^2}{s_1^4/(n_1^2(n_1-1)) + s_2^4/(n_2^2(n_2-1))}. \tag{12}$$

Here, n_1 and n_2, $\overline{x}_1$ and $\overline{x}_2$, and s_1^2 and s_2^2 are the sample size, the sample mean, and the unbiased sample variance, respectively, of the two sets. The statistical test for the difference between $\text{SMR}(\text{LCP} \in j)$ in prior and posterior periods could be done by applying the two-sided tests under the null hypothesis of $\mu_1 - \mu_2 = 0$ at some significance level α. In our case, n_1 and n_2, $\overline{x}_1$ and $\overline{x}_2$, and s_1^2 and s_2^2 are $N(\text{LCP} \in j)$, $\text{SMR}(\text{LCP} \in j)$, and the unbiased variance of SMR_{min} at bin j, respectively, for posterior (suffix 1) and prior (suffix 2) periods.

Some associated changes are made to **Page 28045, line 17**:

The test statistic of the difference (see Appendix A1 for details) is shown in Fig. 5(d) indicating ...

and the figure caption of Figs. 5 and 6 referring to the Appendix.

- **Figure 5**. Horizontal distribution of LCP-event probability, $P(\text{LCP} \in j)$, estimated from the TST trajectories initialized on 400 K in (a) September 1998 and 1999 (prior to the drop) and (b) September 2000, 2001 and 2002 (posterior to the drop). The probabilities are estimated in 10° by 10° longitude-latitude bin as the number of LCPs experienced by all TST air parcels inside the bin divided by the total number of TST parcels used for the calculation ($N(\text{LCP} \in j)/N_{\text{TST}}$). Panels (c) and (d) are the difference of probabilities between the two (posterior minus prior to the drop) and the values of test statistic (T_1 of Appendix A1), respectively. The colored bins indicate that the difference is statistically significant at the significance level of 1 % or higher. Those bins shown in white indicate there found no LCP event in (a) and (b), while the difference is not statistically significant in (c) and (d). See Appendix for the details of statistical tests.

- **Figure 6**. The same as Fig. 5 except that the ensemble mean values of SMR_{min} are illustrated on the bin-by-bin basis ($\text{SMR}(\text{LCP} \in j)$). The test statistic shown in (d) is T_2 of Appendix A2. See Appendix for the details.

Comment: line 8: "leading to a reversal of the zonal gradient of SMR_{min} over the equator" ... I do not understand this sentence.

Reply: This part of the sentence has been deleted.

Comment: Page 28048, line 21: How can the contribution from the Tibetan high and the thermal forcing from the ocean to the SWV drop be quantified by a "projection of the H2O entry values onto bins in the tropics"? I don't understand this sentence.

Reply: The sentence has been revised as follows:

- **Page 28048, lines 22 to 25**: the modulations of the Tibetan high and ... distributed in the tropics (Fig. 7).

has been changed to

the modulations of the Tibetan high and the TTL circulation driven by the thermal forcing from the equatorial ocean. The regional contribution to $[\text{H}_2\text{O}]_{\text{e}}$, quantified by $E(\text{LCP} \in j)$, shows distinct decrease in two regions; one over the Bay of Bengal and the other over the equator in the western tropical Pacific (Fig. 7(c)). The former will be related to the weakening of Tibetan high, while the latter may imply the modulation of the Matsuno-Gill pattern (Matsuno, 1966; Gill, 1980), although these will not be independent between each other.

9. **Comment:** Page 28049, line 5: "without taking the average". I do not understand what you intended to calculate.

Reply: Each panel of Figure 9 is the averaged distribution either before the drop or after the drop. The features commonly appear in each of the months depending on the category either prior or posterior to the drop even if the averages are not taken among years. The sentences have been revised as follows:

- **Page 28049, lines 4 to 7**: The corresponding features appear basically the same ... with the intensity weaker in the latter (2000/2001/2002).

has been changed to

We can see the Tibetan anticyclone in the height field of both periods (left) with the intensity weaker in the latter (2000, 2001 and 2002) than in the former (1998 and 1999). This feature appears basically the same in individual monthly mean values of August depending on the category either prior or posterior to the drop.

Comment: Page 28049, lines 23-29: I cannot follow your description of Figure 10.

Reply: Figure 10 has been redrawn to make the important point clearer. The sentences are revised as follows:

> - **Page 28049, lines 23 to 27**: The difference between the longitudes of warm SST core ... to underlying convective heating (Hatsushika and Yamazaki, 2003).
>
> has been changed to
>
> The possible connection of the water drop in 2000 to the modified SST distribution has been discussed by Rosenlof and Reid (2008). They found the correlation coefficients between tropopause temperature and SST are quite small "if one correlates times prior to 2000, or after 2001" separately, but a large negative correlation coefficient of – 0.44 appears if one correlates the entire time period which, they say, is "exclusively a consequence of the decrease in tropical tropopause temperatures of $\sim 2°$C in $171° - 200°$ longitude band coincident with an increase in SSTs of 0.4°C in the $139° - 171°$ tropical longitude band." The longitudinal difference between the warm SST core and the temperature minimum near the tropopause will be due to the eastward tilt of cold region associated with a steady Kelvin wave response to underlying convective heating (Hatsushika and Yamazaki, 2003). Thus the notion by Rosenlof and Reid (2008) suggests that the SWV drop in 2000 is driven by some dynamical process that accompanies the generation of Matsuno-Gill pattern. This is consistent with the idea that the modified SST distribution is one of the key processes that drove the water drop in the year 2000.

10. **Comment:** Page 28050, lines 1-3: I doubt your conclusion drawn from Fig. 7, namely that the TTL temperature in the Central Pacific is not the cause of the water vapour drop. I think that this interpretation is not supported by the results of Figure 7. Please consider that the cooling in 2001/2002 is distributed over the whole tropical belt, as Figure 9 shows.

    Reply: This point has been already discussed in the reply to item 3 of Specific comment. The sentences are revised as follows:

    > - **Page 28049, line 29 to page 28050, line 3**: The important point in our analysis is that ... by way of the Bay of Bengal and the western tropical Pacific (Fig. 7).
    >
    > has been changed to
    >
    > The important point in our analysis is that the decrease of SMR(LCP$\in j$), albeit widely distributed and remarkable in the tropics (Figs. 6 and 9), is not enough to explain the drop of $[H_2O]_e$ if we recognize the dipole structure, that is, the paired increase and decrease, in $E(\text{LCP} \in j)$ over the equatorial Pacific (Fig. 7). The modified pathway of TTL trajectories, resulted in the reduction of LCP probabilities over the Bay of Bengal and the western tropical Pacific (Fig. 5), is quite important.

11. **Comment:** Discussion section: As far as I understand the following two sentences contradict each other:

    Page 28050 line 1ff: "The important point in our analysis is that the drop of H2O does not come from the decrease of TTL temperature in the Central Pacific but that from the the water transport by way of the Bay of Bengal and the Western tropical Pacific."

    and

    Page 28052 line 6: "The correspondence to the change in the SST distribution ... suggests that the drop and the subsequent low values of H2O are brought about by the eastward expansion of warm SST region to the central Pacific through reduced water entry to the stratosphere."

    Could you please clarify?

    Reply: The former sentence has been replaced as written above. The latter is revised as follows:

    > - **Page 28052, line 6ff**: The correspondence to the change in the SST distribution, the time of occurrence, and the persistency of phenomenon suggest that the drop and the subsequent low values of $[H_2O]_e$ are brought about by the reduced water entry to the stratosphere mainly through the Bay of Bengal (in boreal summer) and the

Western tropical Pacific. The dipole pattern in $E(\mathrm{LCP} \in j)$ over the equatorial Pacific (Figs. 7 and 12) is suggestive of an eastward shift of Matsuno-Gill pattern related to the eastward expansion of warm SST region to the central Pacific.

12. **Comment:** Figure 5: The caption of this figure is not at all comprehensible from the beginning of "The difference of probabilities...". Please give details of the computational method either in the main text or in an appendix. For instance, describe what is considered in the Binomial distributions and how you determined their parameters. What do you mean with Gauss transformation? Is it simply the fact that the Binomial approaches a Gaussian for a large number of data?

    Reply: The details of the computational method have been written in the main text (Reply to item 2 of Specific comments). The issues such as binomial distributions and Gauss transformation are written in Appendix. The caption of Figure 5 is revised as is written in item 8 above.

Technical corrections:

1. **Comment:** Figures 5/6/7: please describe the respective month and year on top of the figures, then it is easier to follow the description in the text.

    Reply: Done.

2. **Comment:** Figure 9/10: color bar is missing.

    Reply: The color bar is found at the top in Figure 9. Figure 10 has been rewritten in monochromatic fashion and no longer needs color bar.

3. **Comment:** Figure 12: select a more appropriate color bar to display the results for the upper and middle figure.

    Reply: The color code of Figure 12 is set exactly the same as that of Fig. 7 so that we could easily compare between the two. Thus the color bar is kept intact.

Manuscript prepared for Atmos. Chem. Phys.
with version 2015/04/24 7.83 Copernicus papers of the LaTeX class copernicus.cls.
Date: 18 December 2015

A Lagrangian description on the troposphere-to-stratosphere transport changes associated with the stratospheric water drop around the year 2000

F. Hasebe[1,2] and T. Noguchi[2,a]

[1]Faculty of Environmental Earth Science, Hokkaido University, Sapporo, Japan
[2]Graduate School of Environmental Science, Hokkaido University, Sapporo, Japan
[a]now at: Human Asset Management and Corporate Affairs Unit, FUJITSU FSAS INC., Kawasaki, Japan

Correspondence to: F. Hasebe (f-hasebe@ees.hokudai.ac.jp)

Abstract. ~~Stratospheric water vapor is known to have decreased suddenly~~ The sudden decrease of stratospheric water vapor at around the year 2000 to 2001 ~~after a prolonged increase through the 1980s and 1990s.~~ is relatively well accepted in spite of the difficulty to quantify the long-term variations. This stepwise change is studied by examining the entry value of water to the stratosphere ($[H_2O]_e$) and some Lagrangian diagnostics of dehydration taking place in the Tropical Tropopause Layer (TTL). The analysis is made using the backward kinematic trajectories initialized every ~ 10 days since January 1997 till December 2002 on 400 K potential temperature surface in the tropics. The $[H_2O]_e$ is estimated by the ensemble mean value of the water saturation mixing ratio (SMR) at the Lagrangian cold point (LCP) where SMR takes minimum (SMR_{min}) in the TTL before reaching the 400 K surface. The drop in $[H_2O]_e$ is identified to have occurred in September 2000. The horizontal projection of September trajectories, tightly trapped by anticyclonic circulation around Tibetan high, shows eastward expansion since the year 2000. Associated changes are measured by three-dimensional bins, each having the dimension of 10° longitude by 10° latitude within the TTL. The probability distribution of LCPs shows appreciable change exhibiting a composite pattern of two components: (i) the dipole structure consisting of the decrease over the Bay of Bengal and Malay Peninsula and the increase over the northern subtropical western Pacific and (ii) the decrease over the equatorial western Pacific and the increase over the central Pacific almost symmetric with respect to the equator. The SMR_{min} shows general decrease in the tropics with some enhancement in the central Pacific. The expectation values, defined by the multiple of the probability of LCP events and the ensemble mean values of SMR_{min}, are calculated on each bin for both periods prior and posterior to the drop. These values are the spatial projection of $[H_2O]_e$ on individual bin. The results indicate that the drop is brought about by the decrease of water transport borne by the air parcels having experienced the LCP over the Bay of Bengal and the western tropical Pacific. The

former is related to the eastward expansion of the anticyclonic circulation around the weakened Tibetan high, while the latter will be linked to the eastward expansion of western tropical warm water to the central Pacific. This oceanic surface forcing may be responsible also for the modulation of dehydration efficiency in the successive northern winter. The drop in September 2000 and the sustained low values thereafter of $[H_2O]_e$ are thus interpreted as being driven by the changes in thermal forcing from the continental and oceanic bottom boundaries.

1 Introduction

Stratospheric water vapor (SWV) observed by balloon-borne hygrometers exhibits gradual increase in the 1980s and 1990s (Oltmans and Hofmann, 1995; Oltmans et al., 2000) followed by a stepwise drop at around the year 2000 (Scherer et al., 2008; Fujiwara et al., 2010). Since SWV has a positive radiative forcing as a greenhouse gas (Shindell, 2001), its possible increase during the two decades could have caused enhanced surface warming by about 30 % as compared to that without taking this increase into account, while the subsequent drop could have slowed down the surface warming by about 25 % from about 0.14 to 0.10 °C per decade (Solomon et al., 2010). The cause and mechanism of this stepwise change have been fluently discussed (e.g., Randel et al., 2006; Rosenlof and Reid, 2008; Bönisch et al., 2011; Fueglistaler, 2012; Fueglistaler et al., 2014; Dessler et al., 2014). While constructing a reliable long-term SWV record is still a challenge (Hegglin et al., 2014), the understanding of a possible stepwise change in SWV is required in assessing possible modulation of the Brewer–Dobson circulation under global warming.

The variation of SWV is driven dynamically by the troposphere-to-stratosphere transport of water and chemically by the oxidation of methane. The dynamical control is mostly associated with the efficiency of dehydration functioning on the air mass advected in the TTL (Holton and Gettelman, 2001; Hatsushika and Yamazaki, 2003). ~~The~~ The Lagrangian description of the transport processes in the tropical troposphere to the stratosphere using trajectory calculations proved to be quite effective not only in the reproduction of SWV variations ~~by using the Lagrangian temperature history along the trajectories has proven quite effective,~~ but also in the characterization of the dehydration processes in the TTL (e.g., Bonazzola and Haynes, 2004; Fueglistaler et al., 2004, 2005; Dessler et al., 2014) even though the quantitative estimation of the water amount entering the stratosphere requires detailed consideration dealing with aerosols and ice particles (ice nucleation and sublimation processes, supersaturation, and deposition and precipitation of ice particles) as well as the minute description of meteorological conditions (subgrid-scale variabilities, intrusion of deep convection into advected air parcels, and irreversible mixing due to breaking waves along with the ambiguity in the analysis field).

Here, we discuss the cause of the stepwise drop in SWV by making the analysis of the entry mixing ratio of water to the stratosphere ($[H_2O]_e$) with the aid of some Lagrangian diagnostics of

TTL dehydration such as the preferred advection pathways in the TTL, the location in which water saturation mixing ratio (SMR) takes minimum along each trajectory (Lagrangian cold point; LCP) together with ~~its occasional~~ the minimum value ($\mathrm{SMR_{min}}$) before entering the stratosphere (Sect. 3). The backward kinematic trajectories initialized on 400 K potential temperature surface in the tropics, similar to those of Fueglistaler et al. (2005), are used. The calculations cover the period from January 1997 to December 2002. The statistical features of the LCP and $\mathrm{SMR_{min}}$ are analyzed for the 90 day trajectories in which the air parcels experienced LCP in the TTL (Sect. 2). The analysis is focused on the examination of the entry value of water to the stratosphere, meaning that any contribution from the recirculation within the stratosphere (ST) and the sideway entry of water to ST without taking the LCP in the TTL are intentionally left out of the scope. Detailed examinations on the driving mechanism itself are left for future studies. ~~However, it will reveal the direct cause~~ However, such a restriction will serve to focus our investigation on some specific processes that may have led to the SWV drop in Lagrangian framework. This approach has ~~the advantages~~ an advantage over Eulerian description because the drop in SWV does not necessarily mean TTL cooling conveniently described in Eulerian framework. For example, it might simply reflect the change in the proportion of air parcels that have passed the coldest region in the TTL. Conversely, any extreme cooling does not necessarily result in enhanced dehydration as long as the air parcels do not experience LCP event in that region. We will try to describe a hypothetical story on the cause of the stepwise drop of SWV through the discussion of the results in Sect. 4. Conclusions are placed in Sect. 5.

2 Method of analysis

2.1 Trajectory calculations

The method of estimating $[\mathrm{H_2O}]_\mathrm{e}$ in the present study is similar to that of Fueglistaler et al. (2005). $[\mathrm{H_2O}]_\mathrm{e}$ at time t is estimated as the ensemble mean value of $\mathrm{SMR_{min}}$ along 90 day backward kinematic trajectories initialized at t. ~~The~~ The backward trajectory calculations are started from uniformly distributed gridpoints (every 5.0° longitude by 1.5° latitude) within 30° N and S from the equator on 400 K potential temperature surface~~, which results in 2952 initialization points in total for single calculation. The calculations are started from~~ . The initializations are made on the 5th, 15th, and 25th of every month during the period since January 1997 till December 2002 relying on the European Centre For Medium-Range Weather Forecasts ERA Interim dataset (Dee et al., 2011). The number of initialization points is 2952 for a single calculation resulting in 8856 for the estimation of monthly values. This number compares well with that of the reduced set of trajectories in the study on the sensitivity of number of trajectories by Bonazzola and Haynes (2004) and turned out to be enough to derive statistically significant results as can be seen later in Section 3. All meteorological variables ~~on the 60-layer~~ given on 60 model levels have been ~~converted~~ interpolated to those on 91 pressure levels keeping the horizontal resolution of 0.75° by 0.75° longitude–latitude grid-

points prior to calculations. The time step has been set to 30 minutes, similar to 36 minutes taken by Bonazzola and Haynes (2004), by applying spatiotemporal interpolations to the 6-hour interval ERA Interim dataset. As for the limitation and caution of this method, see, for example, the pioneering studies by Fueglistaler et al. (2004) and Bonazzola and Haynes (2004).

2.2 Selection of trajectories relevant to TTL dehydration

The meridional projections of the backward trajectories extracted from those initialized on 15 January 1999 are shown in Fig. 1. The top and bottom diagrams are the same except that pressure (top) and potential temperature (bottom) are taken as the ordinate. The asterisks in red indicate the location of the LCP while those in green are the termination point of trajectory calculations (90 days before initialization at the longest). In case the backward extension of the trajectories hit the surface of the earth, the calculations are terminated at that point, and those portions of the trajectories immediately before the surface collision are used for the analysis. The migration of air parcels depicted in the trajectories is roughly categorized into three major branches: quasi-isentropic advection in the TTL and the lower stratosphere (LS), vertical displacement in the troposphere due to diabatic motion resolvable in grid-scale velocity field, and quasi-isentropic migration in the troposphere. We can see many air parcels are traced back to the troposphere representing the tropical troposphere-to-stratosphere transport (TST), while some portion of the trajectories remain in the LS and/or reach the tropical 400 K surface by taking the sideways without making excursions in the TTL. All non-TST trajectories are removed from the following analysis to focus our discussion on the modulation of $[\mathrm{H_2O}]_\mathrm{e}$. For the sake of clarity, the TST particles in the present study are defined as a subset of those particles traceable down to 340 K having recorded LCP in the TTL. For the application of this LCP condition to our trajectories, we introduce the Lagrangian definition of the TTL to assure internal consistency of the analysis.

The motion of air parcels ascending in the tropical troposphere is characterized by rapid convective up-lift that accompanies latitudinal migration associated with the seasonal displacement of the Inter-Tropical Convergence Zone. Up in the TTL, on the other hand, the diabatic ascent is driven by radiative heating, in which the seasonal migration with respect to latitude is much smaller than that in the troposphere because the dynamical field generated by the thermal forcing at the bottom boundary retains relatively high symmetry with respect to the equator. By translating these features into the characteristics of trajectories, we derive a definition of the TTL in a Lagrangian fashion.

Figure 2 on the top illustrates the vertical distribution of the proportion of trajectories categorized on a daily basis as "fast" ascending air parcels. The required rate for the fast ascent is empirically set to more than 0.2 K in potential temperature within 1 time step (30 min), that is, the condition for θ K isentrope is met if the air parcel crosses θ K surface from below $\theta - 0.1$ K to above $\theta + 0.1$ K in 30 min. We can see that the proportion of the fast diabatic ascent thus defined takes maximum at around 340 K in the troposphere and minimum at around 355 K. The proportion of such "fast" air

parcels reduces above the level of main outflow and ~~rapidly decays~~ rapidly goes to near zero toward the level of zero net radiative heating in the TTL. Above this level, the air parcels are diabatically lifted up by radiative heating and further pumped-up by dissipating planetary waves in the midlatitude stratosphere (Holton et al., 1995). The alternation of the primary forcing that drives diabatic ascent is also seen from the bottom panel of Fig. 2, which shows the seasonal migration of the latitudinal position of the trajectories traceable to down below 340 K averaged for (blue) January, (green) April, (yellow) July, and (red) October. The altitude of the kink at around 355 K suggests that the influence of tropical convective motion almost ceases at this level and the diabatic forcing gradually shifts to radiative heating in the TTL and above.

The diagnostic features depicted in Fig. 2 agree that the bottom of the TTL would be most properly defined at 355 K potential temperature level for our study. In the following analysis, we make use of TST trajectories defined by the air parcels that have ascended from the lower troposphere below 340 K isentrope experiencing the LCP in the TTL, which is defined by the layer between the isentropic levels 355 and 400 K within 30° N and S from the equator.

3 Results

3.1 The drop in $[H_2O]_e$

The calculations are made on a monthly basis using the three initialization days (5th, 15th and 25th of each month) at a time. The following description refers to a specific month omitting the suffix for time. Let start by assuming that the minimum saturation mixing ratio along i-th TST trajectory ($i = 1, \cdots, N_{\mathrm{TST}}$) is denoted by $\mathrm{SMR}_{\mathrm{min}\,i}$. The entry value of water to the stratosphere $[H_2O]_e$ is defined as the ensemble mean value of $\mathrm{SMR}_{\mathrm{min}}$ as in Fueglistaler et al. (2005):

$$[H_2O]_e = \frac{1}{N_{\mathrm{TST}}} \sum_{i}^{N_{\mathrm{TST}}} \mathrm{SMR}_{\mathrm{min}\,i}. \quad (1)$$

The evolution of the entry value of water to the stratosphere as modeled in $[H_2O]_e$ time series is shown in Fig. 3. The top panel is the sequential change in the monthly ensemble mean value of $[H_2O]_e$ estimated from the TST air parcels during the period between January 1997 and December 2002. We can see the decrease of the seasonal maxima in boreal summer in 2000. The seasonal minima in boreal winter, on the other hand, show larger values in January–February 2000 as compared to those in 1999, 2001, and 2002 and thus the drop in $[H_2O]_e$ is not quite obvious. As the six-year time series is not long enough to define climatology and anomalies from it, we simply view the interannual variations on the basis of each calendar month. The bottom panel of Fig. 3 is the same as the top except that the data points are connected by each calendar month. When viewed in this way, the drop in the year 2000 of about 1 ppmv shows up in the time change in September (marked by 9), October (10), November (11), and December (12). Similar drop continues to January (1) and

the successive months in 2001. As there is little difference between those in August 1999 and 2000, we may well conclude that the drop in $[H_2O]_e$ occurred in September 2000. Considering the time period required for the air parcels to make excursion in the TTL, we may interpret that the change in the characteristics of dehydration has been initiated in the boreal summer of 2000. The maxima of $[H_2O]_e$ in January through June 1998 are related to the strong El Niño as is discussed later in Sect. 4.

3.2 Horizontal projection of the TST trajectories

As the first step of examining the change in the characteristics of TTL dehydration initiated in northern summer of 2000, Fig. 4 illustrates the horizontal projection of TST trajectories within the layer between the isentropes 360 and 370 K extracted from those initialized in September 1999 (top) and 2000 (bottom). In spite of the equatorially symmetric assignment of the initialization points on 400 K potential temperature surface, the trajectories in the TTL are highly asymmetric with respect to the equator and clustered mostly in the northern subtropics. The dense population of the trajectories shows that the air parcels are largely trapped by Tibetan high in the region between 30° W to 150° E and 0 to 45° N. Comparison between the two, representing September trajectories prior and posterior to the drop, respectively, reveals that the circulation of air parcels around the Tibetan high is loosely tied to the center in the latter period, resulting in the expansion of the anticyclonic circulation branch mostly to the east accompanied by the spread-out of the trajectories farther to the Southern Hemisphere in the latter. This modal shift in the trajectories initialized in September occurs in the year 2000 and continues at least through 2001 and 2002 (not shown).

3.3 Statistical distribution of the LCP

The shift in the circulation pattern of air parcels is not enough to characterize the modification of dehydration efficiency in the TTL. ~~discuss the monsoon circulation during boreal summer in the context of the influence of northern midlatitude on the TTL. The horizontal structure of ozone and water vapor on 390potential temperature surface suggests an intrusion of the ozone-rich midlatitude air into the TTL possibly contributing to the TTL hydration during boreal summer. For the purpose of identifying the~~ To quantify the change in the ~~dehydration efficiency associated~~ LCP distribution associated with the modal shift seen in Fig. 4, the numbers of LCPs are counted by every 10° longitude-latitude bin in the tropics. The probabilities of LCPs are estimated for each bin by dividing the LCP counts by the total number of TST trajectories.

Let assume that i-th TST trajectory ($i = 1, \cdots, N_{\mathrm{TST}}$) takes minimum saturation mixing ratio ($\mathrm{SMR}_{\mathrm{min}\,i}$) at bin j ($j = 1, \cdots, M$), that is, the Lagrangian cold point (LCP) for i-th TST trajectory

is found at bin j. If we denote the number of LCP events at bin j as $N(\mathrm{LCP} \in j)$,

$$N_{\mathrm{TST}} = \sum_{j}^{M} N(\mathrm{LCP} \in j). \tag{2}$$

Because some trajectories do not satisfy the TST condition in general, $N_{\mathrm{TST}} \leq N$, where N is the total number of initialization points used for the calculation. The probability of LCP events at bin j, $P(\mathrm{LCP} \in j)$, is defined by

$$P(\mathrm{LCP} \in j) = \frac{N(\mathrm{LCP} \in j)}{N_{\mathrm{TST}}}, \tag{3}$$

so that the normalization condition $\sum_{j}^{M} P(\mathrm{LCP} \in j) = 1$ holds.

The top two panels of Fig. 5 show the horizontal distributions of ~~the probabilities of LCP events thus obtained~~ $P(\mathrm{LCP} \in j)$ thus defined for those trajectories initialized in September 1998 and 1999 (~~top~~a; prior to the drop) and September 2000, 2001 and 2002 (~~second panel~~b; posterior to the drop). ~~The spatial maximum during the period prior to the drop is found~~ Because N_{TST} is different among individual September, N_{TST} for each month has been used as a weight in taking the averages. In other words, the calculations are made by combining the trajectories of two or three prior- or posterior-months together for the illustrations. To be more specific, the TST trajectories of September 1998 and 1999, selected from $N = 2952 \times 3 \times 2$ trajectories, are combined together for the illustration of Fig. 5(a), while those of September 2000, 2001, and 2002, selected from $N = 2952 \times 3 \times 3$ trajectories, are used for Fig. 5(b). The comparison between the two will shed light on the change in "the sampling effect" of Bonazzola and Haynes (2004). The spatial distribution is characterized by the maxima over the Bay of Bengal and Malay Peninsula ~~with the~~ accompanied by a ridge extending to South China Sea~~(top).~~. It is interesting to note some similarity in the location to the spatial maxima of the first encounter of backward trajectories to 370 K isentrope for June to August 1999 shown by Bonazzola and Haynes (2004). During the period posterior to the drop (~~second panel), this maximum shows~~ Fig. 5(b)), the maxima show eastward expansion as far as 150° E. There also appears some increase in the Central Pacific covering both northern and southern subtropics crossing over the equator. These two components appear clearer in the difference field shown in ~~the third panel.~~ Fig. 5(c). Those bins shown in blue (red) indicate the decrease (increase) of the LCP probabilities in the posterior period. The test statistic of the difference ~~transformed to the standard Gaussian distribution~~ (see Appendix A1 for details) is shown in ~~the bottom panel of the figure~~ Fig. 5(d) indicating the region in which the differences are statistically significant at the significance level of 1 % or higher. It is interesting to note that, in addition to the dipole structure associated with the eastward expansion of the Tibetan anticyclone, the probabilities show significant decrease over the equator at around 130 to 140° E and increase in wider area almost symmetric with

respect to the equator (160° E to 160° W and 10° S to 10° N). This structure will be discussed further in Sect. 4.

3.4 Statistical change in the SMR_{min}

The increase of the LCP events in some bins does not necessarily mean enhanced dehydration over there. The next step is to examine the change in the SMR_{min}. This corresponds to focus on the change in "the temperature effect" of Bonazzola and Haynes (2004). Simultaneous with counting the LCP events, the values of SMR at the time of each LCP event (SMR_{min}) have been summed-up to calculate the average for each bin. The ensemble mean value of SMR_{min} at bin j, SMR(LCP$\in j$), is defined by

$$\mathrm{SMR}(\mathrm{LCP} \in j) = \frac{1}{N(\mathrm{LCP} \in j)} \sum_{i}^{\mathrm{LCP}\in j} \mathrm{SMR}_{\mathrm{min}\,i}, \tag{4}$$

where $\sum_{i}^{\mathrm{LCP}\in j}$ indicates the sum with respect to the subset of TST trajectories that take LCP at bin j.

Figure A2 is the same as Fig. 5 except that ~~the ensemble mean SMR_{min} are~~ SMR(LCP$\in j$) is illustrated rather than ~~the probability of LCP events.~~ $P(\mathrm{LCP} \in j)$. We can see that the averages of SMR_{min} in the tropics are roughly smaller in the eastern than in the western hemisphere accompanying a broad minimum of about 3.5 to 3.7 ppmv over the maritime continent during the period prior to the drop (~~top~~)Fig. A2(a)). The values show general decrease in the tropics with some enhanced drop in the central Pacific reaching less than 3.0 ppmv in the period posterior to the drop (~~second panel from the top), leading to a reversal of zonal gradient of SMR_{min} over the equator~~Fig. A2(b)). The gross features correspond well to the horizontal distribution of the LCP-averaged SMR of July/August 2001 estimated by Fueglistaler et al. (2004). The difference between the two (~~third panel~~)periods (Fig. A2(c)), together with the statistical significance (~~bottom~~)Fig. A2(d)), confirms the pronounced decrease of SMR_{min} in the central Pacific after 2000. On the other hand, the change of SMR_{min} associated with the east-west dipole structure is not so remarkable in terms of the difference of SMR_{min}, although the tendency is the same.

3.5 Statistical change in the expectation values

While the differences of SMR_{min} appear smaller over the Bay of Bengal and Malay Peninsula than over the central Pacific, the comparisons based only on the changes in SMR_{min} (LCP$\in j$) could be misleading, because the ~~probabilities of LCP events~~ values of $P(\mathrm{LCP} \in j)$ are much higher in the former than in the latter (Fig. 5). ~~Figure A2 shows the horizontal distribution of the expectation value of~~ The expectation value for bin j, $E(\mathrm{LCP} \in j)$, is defined by the multiple of $P(\mathrm{LCP} \in j)$ and SMR(LCP$\in j$) to quantify the contribution of each bin to $[H_2O]_e$~~estimated by multiplying the probability of LCP events (Fig. 5) and the ensemble mean SMR_{min} (~~. The sum of $E(\mathrm{LCP} \in j)$ with

respect to all bins reduces to

$$\sum_{j}^{M} E(\mathrm{LCP} \in j) \approx \sum_{j}^{M} P(\mathrm{LCP} \in j) \times \mathrm{SMR}(\mathrm{LCP} \in j) \tag{5}$$

$$\approx \sum_{j}^{M} \frac{N(\mathrm{LCP} \in j)}{N_{\mathrm{TST}}} \times \frac{1}{N(\mathrm{LCP} \in j)} \sum_{i}^{\mathrm{LCP} \in j} \mathrm{SMR}_{\min i} \tag{6}$$

$$\approx \frac{1}{N_{\mathrm{TST}}} \sum_{j}^{M} \sum_{i}^{\mathrm{LCP} \in j} \mathrm{SMR}_{\min i} \tag{7}$$

$$\approx \frac{1}{N_{\mathrm{TST}}} \sum_{i}^{N_{\mathrm{TST}}} \mathrm{SMR}_{\min i}. \tag{8}$$

This is the entry value of water to the stratosphere $[\mathrm{H_2O}]_{\mathrm{e}}$ (Eq. (1)) shown as a time series in ~~A2) together for each bin.~~ 3. $[\mathrm{H_2O}]_{\mathrm{e}}$ is thus decomposed of the sum of $E(\mathrm{LCP} \in j)$, which is interpreted as the contribution of bin j to $[\mathrm{H_2O}]_{\mathrm{e}}$. What is important here is that it is neither $P(\mathrm{LCP} \in j)$ nor SMR(LCP$\in j$) but the product between the two, $E(\mathrm{LCP} \in j)$, that is directly responsible for composing the value $[\mathrm{H_2O}]_{\mathrm{e}}$. By comparing the distribution of $E(\mathrm{LCP} \in j)$ between the two periods, prior and posterior to the drop, we can see how the drop in $[\mathrm{H_2O}]_{\mathrm{e}}$ is brought about by the change of water transport from individual region.

Figure A2 shows the horizontal distribution of $E(\mathrm{LCP} \in j)$. This corresponds to the projection of $[\mathrm{H_2O}]_{\mathrm{e}}$ onto each bin. We can see that the September values of $[\mathrm{H_2O}]_{\mathrm{e}}$ are mostly projected to the Bay of Bengal and Malay Peninsula before the drop (~~top panel)~~Fig. A2(a)). The contribution from this core area remains dominant during the posterior period (~~middle panel).The reductions ttom panel)are mainly due to the decreases of the LCP-event probability (Fig. 5)cooperated by the reduced ensemble mean $\mathrm{SMR}_{\min}$~~ Fig. A2(b)). While the reduction of $[\mathrm{H_2O}]_{\mathrm{e}}$ cannot be free from the general cooling (lowering of SMR(LCP$\in j$)) in posterior years over most of the tropics (Fig. A2)~~. The corresponding increase of LCP-event probabilities especially that over the central Pacific has contributed to a slight increase~~ , it is interesting to note the increase of $E(\mathrm{LCP} \in j)$ despite the rease in SMR(LCP$\in j$) over the central Pacific. This is because the increase of $P(\mathrm{LCP} \in j)$ more than compensate for the decrease of SMR(LCP$\in j$) over there. In this sense, it is not appropriate to attribute the cooling over the western and the central Pacific to the drop in $[\mathrm{H_2O}]_{\mathrm{e}}$~~because the magnitude of increase in occurrence frequency prevails~~ . The similarity in the spatial distributions of $P(\mathrm{LCP} \in j)$ and $E(\mathrm{LCP} \in j)$, especially that of the ~~decrease in $\mathrm{SMR}_{\min}$.~~ location of maxima r the Bay of Bengal and Malay Peninsula together with the post 2000 decrease over there and the western tropical Pacific, suggests that the relocation of LCPs (change in $P(\mathrm{LCP} \in j)$) is a leading factor that has caused the drop in $[\mathrm{H_2O}]_{\mathrm{e}}$ in September 2000.

The resultant changes could be interpreted as the composite of two components: (i) the decrease over the Bay of Bengal and (ii) the decrease over the equatorial western Pacific and the increase

over the central Pacific almost symmetric with respect to the equator extending to the subtropical latitudes of both hemispheres. The former is supplemented by slight decrease widespread along the 10° N zonal belt with the exception around 150° E and the central Pacific. These features will be related to the eastward expansion of the anticyclonic circulation around the Tibetan high, while the latter is suggestive of some response to the thermal forcing from the equatorial ocean.

4 Discussion

4.1 Maxima of $[H_2O]_e$ in 1998

We have seen in Fig. 3 that the time series of $[H_2O]_e$ shows maxima in January through June 1998. We excluded these months from our analysis in Sect. 3 because of the influences of strong El Niño. The values of $[H_2O]_e$ in November and December 1997 are larger than those in 1998, which may suggest possible influence of El Niño also in these months. Actually Fueglistaler and Haynes (2005) demonstrated in their Fig. 2 that the trajectory model shows large increase of lower-stratospheric water ($[H_2O]_{T400}$ which takes non-TST trajectories into account in addition to $[H_2O]_e$) associated with El Niño and that the increase is accompanied by the eastward shift of the high density region of LCP. The reason why we regard these facts as little related to the drop of $[H_2O]_e$ in 2000 is briefly discussed here.

For exploration of the reason of such anomalies, the horizontal distributions of LCP are shown for those initialized in February 1997, 1998 and 1999 in Fig. A2. The distributions in February 2000, 2001 and 2002 (not shown) are similar to those of 1997 and 1999. The LCPs in February are commonly distributed almost symmetric with respect to the equator, but the longitudinal distribution is not uniform. High concentration in the western tropical Pacific in 1997 and 1999 (and also in 2000, 2001 and 2002) is suggestive of the strong influence of the warm sea surface temperature (SST) on the LCP distribution. The large scatter extending to the eastern tropical Pacific in 1998 is due to the migration of the large scale convective system to the east associated with the strong El Niño. We have put this anomalous change out of the scope of the present study, because those anomalous values seem to have recovered to normal by the northern summer of 1998 (well before 2000) and there is no reasoning that this strong El Niño is coupled to the drop in $[H_2O]_e$ in 2000. For the objective judgement of the influence of the El Niño, we employ the SST averaged in the region between 90° W and 150° W longitude and 5° S to 5° N latitude (Niño 3 region, Trenberth, 1997). Those months exhibiting the SST anomalies (relative to the 1981-to-2010 climatology) greater than 1.5 times the standard deviation are excluded from the present analysis. Those excluded are the twelve months from June 1997 to May 1998.

4.2 Perspective to the mechanism of the drop

The entry value of water to the stratosphere, $[H_2O]_e$, estimated by the ensemble mean values of SMR_{min} along the TST trajectories shows appreciable decrease in September 2000 (Fig. 3), suggesting some modulation in the dehydration efficiency functioning on the air parcels advected in the TTL during the northern summer of 2000. The horizontal projection of ~~trajectories initialized in September~~ September trajectories, characterized by anticyclonic circulation associated with Tibetan high in the TTL, shows eastward expansion in the year 2000 accompanied by some bifurcation to the Southern Hemisphere (Fig. 4). This modal shift appears as decreases in the probability distribution of the LCP over the Bay of Bengal and the western tropical Pacific (Fig. 5). The SMR averaged on the occasion of LCP events (SMR_{min}) shows general decrease with some enhancement in the central Pacific (Fig. A2). These results suggest two possible components contributing to the sudden drop of $[H_2O]_e$ in September 2000: the modulations of the Tibetan high and the TTL circulation driven by the thermal forcing from the equatorial ocean. The ~~contribution from these two components has been quantified by projecting the~~ regional contribution to $[H_2O]_e$ ~~onto bins distributed in the tropics~~, quantified by $E(\mathrm{LCP} \in j)$, shows distinct decrease in two regions; one over the Bay of Bengal and the other over the equator in the western tropical Pacific (Fig. A2~~).~~ (c)). The former will be related to the weakening of Tibetan high, while the latter may imply the modulation of the Matsuno-Gill pattern (Matsuno, 1966; Gill, 1980), although these will not be independent between each other. The results indicate that the drop is brought about by a response of the TTL circulation to the modulated forcing both from the continental summer monsoon and the equatorial ocean. It is thus quite interesting to take a brief look at the changes in the TTL meteorological fields in Eulerian framework before concluding this study.

Figure 9 illustrates the longitude-latitude section of 100 hPa geopotential height (left) and temperature (right) averaged in August 1998 and 1999 (top) and 2000, 2001 and 2002 (middle). These are the background Eulerian fields having roughly brought about the Lagrangian features described by the top two panels of Figs. 5–A2. ~~The corresponding features appear basically the same if we look at individual August without taking the average.~~ We can see the Tibetan anticyclone in the height field of both periods (left) with the intensity weaker in the latter (2000~~/~~, 2001 ~~/~~and 2002) ~~.~~ than in the former (1998 and 1999). This feature appears basically the same in individual monthly mean values of August depending on the category either prior or posterior to the drop. The expansion of the trajectories after 2000 (Fig. 4), therefore, is the result of loosened grip of air parcels around weakened Tibetan high in the latter years. These features remain the same in September of other years posterior to the drop (not shown). The temperature field (right-hand side) both prior and posterior to the drop appears as the typical pattern of the TTL response to the thermal forcing at the bottom boundary with additional heating to the subtropical Northern Hemisphere (Matsuno, 1966; Gill, 1980). The difference (~~bottom panel)~~Fig. 9(e)) indicates substantial cooling in the northern subtropics at around 150° E and the central Pacific. The latter corresponds to the findings of Rosenlof and Reid (2008) in

which the tropical tropopause temperature in 171 to 200° E longitude band decreased in association with the SWV drop in 2000.

The correspondence of the decrease of the equatorial 100 hPa temperature to the increase of the underlying SST is explored in Fig. 10, which shows the longitude-time section of the equatorial SST averaged between 10° N and S of the equator. We could see the warm SST region in the western Pacific expands to the east in the year 2000, and the contour of 28 °C, the threshold of active convection (Gadgil et al., 1984), during the coldest month of the year crossed the date line in 2001. The difference between the longitudes of The possible connection of the water drop in 2000 to the modified SST distribution has been discussed by Rosenlof and Reid (2008). They found the correlation coefficients between tropopause temperature and SST are quite small "if one correlates times prior to 2000, or after 2001" separately, but a large negative correlation coefficient of – 0.44 appears if one correlates the entire time period which, they say, is "exclusively a consequence of the decrease in tropical tropopause temperatures of ~ 2 °C in 171°–200° longitude band coincident with an increase in SSTs of 0.4 °C in the 139°–171° tropical longitude band." The longitudinal difference between the warm SST core and the temperature minimum near the tropopause , noticed already by , is will be due to the eastward tilt of cold region associated with a steady Kelvin wave response to underlying convective heating (Hatsushika and Yamazaki, 2003). Thus the notion by Rosenlof and Reid (2008) suggests that the SWV drop in 2000 is driven by some dynamical process that accompanies the generation of Matsuno-Gill pattern. This is consistent with the idea that the modified SST distribution is one of the key processes that drove the water drop in the year 2000. The warm condition in the central Pacific continues at least till the end of 2005. The decrease of 100 hPa temperature over the central Pacific is, thus, well correlated to this SST variation. The important point in our analysis is that the the decrease of SMR(LCP$\in j$), albeit widely distributed and remarkable in the tropics (Figs. A2 and 9), is not enough to explain the drop of $[H_2O]_e$ does not come from the decrease of TTL temperature in the central Pacific but that from the water transport by way of if we recognize the dipole structure, that is, the paired increase and decrease, in $E(\mathrm{LCP} \in j)$ over equatorial Pacific (Fig. A2). The modified pathway of TTL trajectories, resulted in the reduction of LCP probabilities over the Bay of Bengal and the western tropical Pacific (Fig. A2). 5), is quite important.

The study by Young et al. (2012), discussing the changes in the Brewer–Dobson circulation during the period 1979 to 2005 by referring to the out-of-phase temperature relationship between the tropics and the extratropics, found no appreciable change around the year 2000. However, the zonally uniform component exhibiting the out-of-phase relationship between the tropics and the extratropics in 100 hPa temperature difference (Fig. 9) is suggestive of some stratospheric contribution to the drop in $[H_2O]_e$ (Randel et al., 2006) through wave-driven pumping (Holton et al., 1995). Actually the analysis of dynamical fields such as eddy heat flux and EP-flux by Fueglistaler (2012) finds a strengthening of the residual circulation qualitatively consistent with the drop of SWV in *October*

2000. Figure 11 shows in color the time-height section of monthly mean vertical wind velocity in the tropics. The seasonal enhancement in the upward motion during northern winter shows up in the lowermost stratosphere. The solid and dashed contours superposed on the vertical velocity field are the zonal wind components depicting the westerly and the easterly phase, respectively, of the quasi-biennial oscillation (QBO). The stagnation of the downward propagation specifically that of the easterly phase of the QBO is noticed in late 1997 to early 1998 and late 2000 to early 2001 at around 40 hPa level. This phase dependency of the stagnant propagation is brought about by the secondary circulation of the QBO in which the upward (downward) motion accompanies the easterly (westerly) shear zone of the QBO (Plumb and Bell, 1982; Hasebe, 1994). What is interesting here is that the enhanced upward motion is found in September and October 2000 blocking the downward propagation of easterlies. The limitation from our use of Eulerian vertical velocity, rather than TEM residual velocity, will be minimal as we focus our discussion in the tropics. Actually the anomalies in the equatorial upwelling at 78 hPa estimated by Rosenlof and Reid (2008) show similar results. Further analysis by Fueglistaler et al. (2014) emphasize that the strengthening of the residual circulation does not last long but continues for a few years around the year 2000. Remembering the time of excursion for air parcels circulating the Tibetan high (Fig. 4), the stratospheric anomalies in October 2000 (Fueglistaler, 2012) appears later than the initiation of the drop in $[\mathrm{H_2O}]_\mathrm{e}$. The difference of one month, albeit small, is large enough to be resolved in the analysis. Then the enhanced upwelling discussed by Fueglistaler et al. (2014) might be the stratospheric response to the tropospheric forcing that modulated the dehydration efficiency in the preceding boreal summer of 2000 rather than the direct cause of the SWV drop. Further studies employing numerical simulations are definitely required. It is worth mentioning here that the enhancement of the Brewer–Dobson circulation may have occurred also in the northern hemispheric branch; the age of northern midlatitude stratospheric air diagnosed by the $\mathrm{CO_2}$ concentration appears shorter than usual in 2002 (Engel et al., 2009, Fig. 3), although the difference is not statistically significant.

4.3 Perspective to the mechanism of sustained low amount of $[\mathrm{H_2O}]_\mathrm{e}$

We have seen some background meteorological fields from Eulerian perspective to interpret the evidences presumably responsible for the drop of $[\mathrm{H_2O}]_\mathrm{e}$ in September 2000 described in Lagrangian framework. The problems not yet answered are what is the specific event (if any) and how is it generated that has triggered the sequence of phenomena that ultimately led to the sudden drop of SWV. In addition, the sustained low values of $[\mathrm{H_2O}]_\mathrm{e}$ after September 2000 need some mechanism that lasts longer than the seasonal time scale, since the modulation of Tibetan high cannot explain the reduction continuing to the successive months in northern winter (Fig. 3).

—Figure 12 is the same as Fig. A2 except that the January projection is illustrated. We can see, in addition to the values generally lower than those in September, the larger values are found in the western tropical Pacific (top and middle panels), Fig. 12(a), (b)), indicating the January values of

~~[~~$\mathrm{H_2O}]_\mathrm{e}$ are controlled by those over the western Pacific. This is consistent with the picture having ~~been~~ presented in numerical simulations (Hatsushika and Yamazaki, 2003). The difference between ~~the~~ two periods ~~(the bottom diagram)~~(Fig. 12(c)) shows decrease over Indonesia and increase over central Pacific during the period posterior to the drop. ~~This pattern in January~~ The former is ~~due~~ to the combination of the decreases in both $P(\mathrm{LCP} \in j)$ and SMR(LCP$\in j$), while the latter ~~is~~ brought about by the ~~combination of the decrease~~ interplay between the increase in $P(\mathrm{LCP} \in j)$ ~~and~~ some decrease of SMR(LCP$\in j$) (not shown). This situation is the same as what we see in ~~S~~september (Section 3.5). The similarity of this pattern, that is, the decrease in the equatorial western ~~P~~acific ~~(increase) of LCP-probability and the slight (enhanced)decrease of~~ $\mathrm{SMR_{min}}$ ~~values over the western (central) Pacific (not shown)~~ over Indonesia) and the increase over the central Pacific, to that ~~of~~ the second component of September response suggests the existence of a common driver of the ~~drop~~ in $[\mathrm{H_2O}]_\mathrm{e}$ irrespective of the season. These evidences suggest the idea that the drop of $[\mathrm{H_2O}]_\mathrm{e}$ ~~in~~ northern winter ~~is due to~~ has resulted from the response of the TTL circulation to the eastward ~~ex~~pansion of the warm water to the central Pacific (Fig. 10) ~~.~~

in such a way that the decrease of $E(\mathrm{LCP} \in j)$ in the western Pacific exceeds the increase of that in the central Pacific.

The correspondence to the change in the SST distribution, the time of occurrence, and the persistency of phenomenon suggest that the drop and the subsequent low values of $[\mathrm{H_2O}]_\mathrm{e}$ are brought about by the ~~eastward~~ reduced water entry to the stratosphere mainly through the Bay of Bengal (in boreal summer) and the Western tropical Pacific. The dipole pattern in $E(\mathrm{LCP} \in j)$ over the equatorial Pacific (Figs. A2 and 12) is suggestive of an eastward shift of Matsuno-Gill pattern related to the eastward expansion of warm SST region to the central Pacific~~through reduced water entry to the stratosphere.~~. Then our hypothetical story may read, the eastward expansion of warm SST region brings about the reduction of $[\mathrm{H_2O}]_\mathrm{e}$ by TST air parcels passing through the western tropical Pacific during northern winter (Fig. 12), while the heating from the modulated SST mentioned above, competing against that over the continent, has led to the modal shift of trajectories during northern summer resulting in the reduced water transport over the Bay of Bengal and the western tropical Pacific (Fig. A2).

The above speculation might end up with some proper explanation on the cause of the eastward expansion of the equatorial warm water to the central Pacific observed in 2000. In this context, it is interesting to see possible occurrence of "El Niño Modoki" characterized by the warm SST event over the central Pacific (W. J. Randel, personal communication, 2015). Actually the time series of normalized ENSO Modoki index of Ashok et al. (2007) turns from prolonged negative to positive towards 2001. It is also interesting to note that the "La Niña-like condition," tied to the surface cooling of the equatorial eastern Pacific, is supposedly responsible for the recent hiatus, the pause of the global-mean surface air temperature ~~rise through the strengthening of ocean heat uptake~~ rise (Kosaka and Xie, 2013; Watanabe et al., 2014). If proved to be true, we may have unveiled another

piece of pathways the internal variability of our climate system could exert on the surface cooling through SST-driven SWV fluctuations.

5 Conclusions

Backward kinematic trajectories, initialized on 400 K potential temperature surface in the tropics, have been employed to describe the stratospheric water drop observed at around 2000 to 2001 from a Lagrangian point of view. The entry value of water to the stratosphere, $[H_2O]_e$, shows appreciable decrease in the trajectories initialized in September 2000 suggesting the change in the TTL dehydration efficiency during the boreal summer of 2000. The following changes are found to be responsible for the drop in $[H_2O]_e$. The reduction of water vapor transported by those air parcels that experienced LCP events in two regions; over the Bay of Bengal and the western tropical Pacific. The reductions are brought about by the decreases in both the LCP-event probability and the ensemble mean SMR_{min} over there. The LCP reduction in the former region is related to the modified migration pathways of air parcels circulating the weakened Tibetan anticyclone, while that in the latter may be a response to eastward expansion of warm water to the central Pacific. This SST modulation seems to be responsible also for the decrease of $[H_2O]_e$ in the successive northern winter. Some indication of stratospheric contribution through intensified pumping appears only intermittent and will be better interpreted as a response to tropospheric forcing changes.

Appendix A: Statistical tests between prior and posterior to the drop

A1 The difference of $P(\mathrm{LCP} \in j)$

Let the random variable, X, is the number of event occurrences in some number of trials, n. The binomial distribution can be used to calculate the probabilities for each of $n+1$ possible values of X ($X = 0, 1, \cdots, n$) if the following conditions are met: (1) the probability of the event occurring does not change from trial to trial, and (2) the outcomes on each of the n trials are mutually independent. These conditions are rarely met, but real situations can be close enough to this ideal that the binomial distribution provides sufficiently accurate representations. The probability that the number of occurrence X is x among n trials, $\Pr(X = x)$, follows the binomial distribution

$$\Pr(X = x) = \begin{pmatrix} n \\ x \end{pmatrix} p^x (1-p)^{n-x}, \quad (x = 0, 1, \cdots, n), \tag{A1}$$

where p is the probability of occurrence of the event.

The statistical test for the difference in the population proportion of two binomial populations, $p_1 - p_2$, could be made as follows. Let the sample size and the sample proportion of the two sets

being n_1 and n_2 and m_1/n_1 and m_2/n_2, respectively. The test statistic, T_1, defined by

$$\sqrt{p^*(1-p^*)(1/n_1+1/n_2)}, \quad p^* = \frac{m_1+m_2}{n_1+n_2},$$

(A2)

follows approximately the standard normal distribution. The statistical test for the difference between $N(\text{LCP} \in j)$ in prior and posterior periods could be done by applying the two-sided tests under the null hypothesis of $p_1 - p_2 = 0$ at some significance level α, where p_1 and p_2 are the population proportion of LCP taking place at bin j in the posterior and prior to the drop, respectively. In our case, n_1 and n_2, and m_1 and m_2, are N_{TST} and $N(\text{LCP} \in j)$, respectively, for posterior (suffix 1) and prior (suffix 2) periods.

A2 The difference of SMR(LCP$\in j$)

The statistical test to be applied is the comparison of the population means of two normal distributions, μ_1 and μ_2, with unknown population variances. This test is sometimes called the Welch's t test. The test statistic, T_2, defined by

$$\sqrt{s_1^2/n_1 + s_2^2/n_2},$$

(A3)

follows the t distribution of the degree of freedom m, where

$$s_1^4/(n_1^2(n_1-1)) + s_2^4/(n_2^2(n_2-1)).$$

(A4)

Here, n_1 and n_2, $\overline{x}_1$ and $\overline{x}_2$, and s_1^2 and s_2^2 are the sample size, the sample mean, and the unbiased sample variance, respectively, of the two sets. The statistical test for the difference between SMR(LCP$\in j$) in prior and posterior periods could be done by applying the two-sided tests under the null hypothesis of $\mu_1 - \mu_2 = 0$ at some significance level α. In our case, n_1 and n_2, $\overline{x}_1$ and $\overline{x}_2$, and s_1^2 and s_2^2 are $N(\mathrm{LCP} \in j)$, SMR(LCP$\in j$), and the unbiased variance of $\mathrm{SMR}_{\min}$ at bin j, respectively, for posterior (suffix 1) and prior (suffix 2) periods.

Acknowledgements. This work is based on the Master of Science Thesis of T. Noguchi submitted to the Graduate School of Environmental Science, Hokkaido University in February 2015. T. Noguchi is grateful to the members of the Graduate School of Environmental Science for the encouragement and discussions through the preparation of his thesis. The discussion with Koji Yamazaki of Hokkaido University is greatly appreciated. The results in part have been presented at the CT3LS Meeting having been held in July 2015. F. Hasebe is grateful to the comments from meeting participants especially W. J. Randel of NCAR and K. H. Rosenlof of NOAA. The authors express hearty gratitudes to S. Fueglistaler (referee) and an anonymous reviewer for helpful and constructive comments. NOAA OI SST V2 data are provided by the NOAA/OAR/ESRL PSD, Boulder, Colorado, USA, from their Web site at http://www.esrl.noaa.gov/psd/. This work was supported by the Japan Society for the Promotion of Science, Grant-in-Aid for Scientific Research (S) 26220101.

References

Ashok, K., Behera, S. K., Rao, S. A., Weng, H., and Yamagata, T.: El Niño modoki and its possible teleconnection, J. Geophys. Res., 112, c11007, doi:10.1029/2006JC003798, 2007.

Bonazzola, M., and Haynes, P. H.: A trajectory-based study of the tropical tropopause region, J. Geophys. Res., 109, D20112, doi:10.1029/2003JD004356, 2004.

Bönisch, H., Engel, A., Birner, Th., Hoor, P., Tarasick, D. W., and Ray, E. A.: On the structural changes in the Brewer–Dobson circulation after 2000, Atmos. Chem. Phys., 11, 3937–3948, doi:10.5194/acp-11-3937-2011, 2011.

Dee, D. P., Uppala, S. M., Simmons, A. J., Berrisford, P., Poli, P., Kobayashi, S., Andrae, U., Balmaseda, M. A., Balsamo, G., Bauer, P., Bechtold, P., Beljaars, A. C. M., van de Berg, L., Bidlot, J., Bormann, N., Delsol, C., Dragani, R., Fuentes, M., Geer, A. J., Haimberger, L., Healy, S. B., Hersbach, H., Hólm, E. V., Isaksen, L., Kållberg, P., Köhler, M., Matricardi, M., McNally, A. P., Monge-Sanz, B. M., Morcrette, J. J., Park, B. K., Peubey, C., de Rosnay, P., Tavolato, C., Thépaut, J. N., and Vitart, F.: The ERA-interim reanalysis: configuration and performance of the data assimilation system, Q. J. Roy. Meteor. Soc., 137, 553–597, 2011.

Dessler, A. E., Schoeberl, M. R., Wang, T., Davis, S. M., Rosenlof, K. H., and Vernier, J.-P.: Variations of stratospheric water vapor over the past three decades, J. Geophys. Res.-Atmos., 119, 12588–12598, doi:10.1002/2014JD021712, 2014.

Engel, A., Möbius, T., Bönisch, H., Schmidt, U., Heinz, R., Levin, I., Atlas, E., Aoki, S., Nakazawa, T., Sugawara, S., Moore, F., Hurst, D., Elkins, J., Schauffler, S., Andrews, A., and Boering, K.: Age of stratospheric air unchanged within uncertainties over the past 30 Years, Nat. Geosci., 2, 28–31, 2009.

Fueglistaler, S.: Stepwise changes in stratospheric water vapor?, J. Geophys. Res., 117, D13302, doi:10.1029/2012JD017582, 2012.

Fueglistaler, S., and Haynes, P. H.: Control of interannual and longer-term variability of stratospheric water vapor, J. Geophys. Res., 110, D24108, doi:10.1029/2005JD006019, 2005.

Fueglistaler, S., Wernli, H., and Peter, T.: Tropical troposphere-to-stratosphere transport inferred from trajectory calculations, J. Geophys. Res., 109, D03108, doi:10.1029/2003JD004069, 2004.

Fueglistaler, S., Bonazzola, M., Haynes, P. H., and Peter, T.: Stratospheric water vapor predicted from the Lagrangian temperature history of air entering the stratosphere in the tropics, J. Geophys. Res., 110, D08107, doi:10.1029/2004JD005516, 2005.

Fueglistaler, S., Abalos, M., Flannaghan, T. J., Lin, P., and Randel, W. J.: Variability and trends in dynamical forcing of tropical lower stratospheric temperatures, Atmos. Chem. Phys., 14, 13439–13453, doi:10.5194/acp-14-13439-2014, 2014.

Fujiwara, M., Vömel, H., Hasebe, F., Shiotani, M., Ogino, S.-Y., Iwasaki, S., Nishi, N., Shibata, T., Shimizu, K., Nishimoto, E., Canossa, J. M. V., Selkirk, H. B., and Oltmans, S. J.: Seasonal to decadal variations of water vapor in the tropical lower stratosphere observed with balloon-borne cryogenic frostpoint hygrometers, J. Geophys. Res., 115, D18304, doi:10.1029/2010JD014179, 2010.

Gadgil, S., Joseph, P. V., and Joshi, N. V.: Ocean-atmosphere coupling over monsoon regions, Nature, 312, 141–143, 1984.

Gill, A. E.: Some simple solutions for heat-induced tropical circulation, Q. J. Roy. Meteor. Soc, 106, 447–462, 1980.

Hasebe, F.: Quasi-biennial oscillations of ozone and diabatic circulation in the equatorial stratosphere, J. Atmos. Sci., 51, 729–745, 1994.

Hatsushika, H. and Yamazaki, K.: Stratospheric drain over Indonesia and dehydration within the tropical tropopause layer diagnosed by air parcel trajectories, J. Geophys. Res., 108, 4610, doi:10.1029/2002JD002986, 2003.

Hegglin, M. I., Plummer, D. A., Shepherd, T. G., Scinocca, J. F., Anderson, J., Froidevaux, L., Funke, B., Hurst, D., Rozanov, A., Urban, J., von Clarmann, T., Walker, K. A., Wang, H. J., Tegtmeier, S., and Weigel, K.: Vertical structure of stratospheric water vapour trends derived from merged satellite data, Nat. Geosci., 7, 768–776, doi:10.1038/ngeo2236, 2014.

Holton, J. R. and Gettelman, A.: Horizontal transport and the dehydration of the stratosphere, Geophys. Res. Lett., 28, 2799–2802, 2001.

Holton, J. R., Haynes, P. H., McIntyre, M. E., Douglass, A. R., Rood, R. B., and Pfister, L.: Stratosphere-troposphere exchange, Rev. Geophys., 33, 403–439, 1995.

Kosaka, Y. and Xie, S.-P.: Recent global-warming hiatus tied to equatorial Pacific surface cooling, Nature, 501, 403–407, 2013.

Matsuno, T.: Quasi-geostrophic motions in the equatorial area, J. Meteorol. Soc. Jpn., 44, 25–43, 1966.

Oltmans, S. J. and Hofmann, D. J.: Increase in lower-stratospheric water vapour at a mid-latitude Northern Hemisphere site from 1981 to 1994, Nature, 374, 146–149, 1995.

Oltmans, S. J., Vömel, H., Hofmann, D. J., Rosenlof, K. H., and Kley, D.: The increase in stratospheric water vapor from balloonborne, frostpoint hygrometer measurements at Washington, D.C., and Boulder, Colorado, Geophys. Res. Lett., 27, 3453–3456, 2000.

Plumb, R. A. and Bell, R. C.: A model of the quasi-biennial oscillation on an equatorial beta-plane, Q. J. Roy. Meteor. Soc., 108, 335–352, 1982.

~~Randel, W. J. and Jensen, E. J.: Physical processes in the tropical tropopause layer and their roles in a changing climate, Nat. Geosci., 6, 169–176, doi:, 2013.~~

Randel, W. J., Wu, F., Vömel, H., Nedoluha, G. E., and Forster, P.: Decreases in stratospheric water vapor after 2001: links to changes in the tropical tropopause and the Brewer–Dobson circulation, J. Geophys. Res., 111, D12312, doi:10.1029/2005JD006744, 2006.

Rosenlof, K. H. and Reid, G. C.: Trends in the temperature and water vapor content of the tropical lower stratosphere: sea surface connection, J. Geophys. Res., 113, D06107, doi:10.1029/2007JD009109, 2008.

Scherer, M., Vömel, H., Fueglistaler, S., Oltmans, S. J., and Staehelin, J.: Trends and variability of midlatitude stratospheric water vapour deduced from the re-evaluated Boulder balloon series and HALOE, Atmos. Chem. Phys., 8, 1391–1402, doi:10.5194/acp-8-1391-2008, 2008.

Shindell, D. T.: Climate and ozone response to increased stratospheric water vapor, Geophys. Res. Lett., 28, 1551–1554, 2001.

Solomon, S., Rosenlof, K. H., Portmann, R. W., Daniel, J. S., Davis, S. M., Sanford, T. J., and Plattner, G.-K.: Contributions of stratospheric water vapor to decadal changes in the rate of global warming, Science, 327, 1219–1223, 2010.

Trenberth, K. E.: The definition of El Niño, B. Am. Meteorol. Soc., 78, 2771–2777, 1997.

Watanabe, M., Shiogama, H., Tatebe, H., Hayashi, M., Ishii, M., and Kimoto, M.: Contribution of natural decadal variability to global warming acceleration and hiatus, Nature Clim. Change, 4, 893–897, doi:10.1038/Nclimate2355, 2014.

Young, P. J., Rosenlof, K. H., Solomon, S., Sherwood, S. C., Fu, Q., and Lamarque, J.-F.: Changes in stratospheric temperatures and their implications for changes in the Brewer–Dobson circulation, 1979–2005, J. Climate, 25, 1759–1772, doi:10.1175/2011JCLI4048.1, 2012.

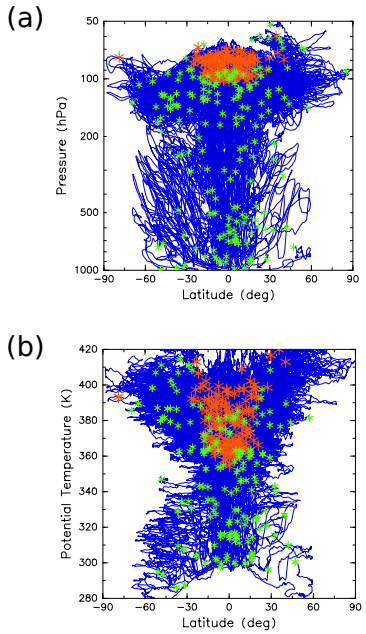

Figure 1. The meridional projections in (~~top~~a) pressure and (~~bottom~~b) isentropic coordinates of 90 day kinematic backward trajectories initialized on 400 K potential temperature surface at 15 January 1999. Initial positions are set at 5.0° longitude by 1.5° latitude gridpoints covering the tropical zone within 30° N and S from the equator. Those shown here are the subsets in which the initial positions are trimmed to 20.0° by 6.0° gridpoints for visual clarity. The asterisks marked in red are the Lagrangian Cold Points, while those in green are the termination points of trajectory calculations. The calculations end up if the backward extension of the trajectories hit the surface of the earth even in less than 90 days before initialization.

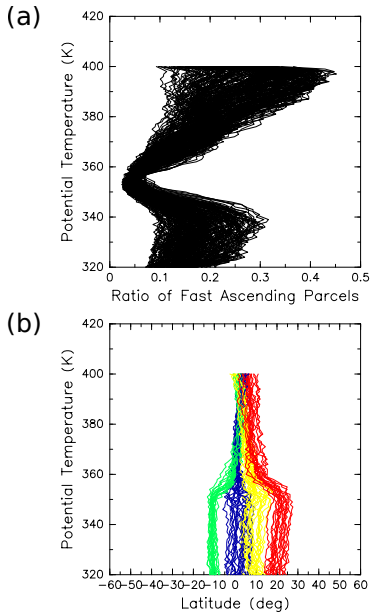

Figure 2. The vertical profiles of (~~top~~a) proportion of the "fast" ascending air parcels and (~~bottom~~b) averaged ascending track diagnosed by 90 day kinematic back trajectories that extends from 400 K to the lower troposphere below 340 K potential temperature surface. The upward motion on θ K isentrope is categorized as "fast" if the air parcel crosses θ K surface from below $\theta - 0.1$ K to above $\theta + 0.1$ K in 30 min. Each line in ~~the top panel~~ (a) shows the daily proportion of trajectories at each isentropic level that correspond to "fast" ascending air parcels. The ascending tracks in ~~the bottom panel~~ (b) are color-coded on a monthly basis (January in blue, April in green, July in yellow, and October in red) to visualize the seasonal migration of the ascending latitude in the tropics.

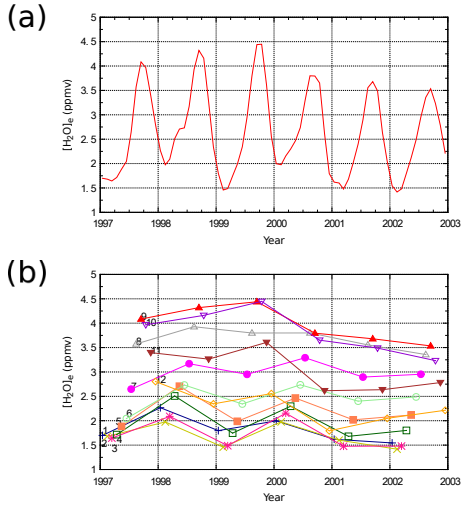

Figure 3. The time series of the ensemble mean values of $[H_2O]_e$ (ppmv) estimated from the TST trajectories initialized on the corresponding month. The data points are connected by sequential month ~~on the top panel~~in (a), while they are linked by each calendar month to visualize interannual variations on a monthly basis in ~~the bottom~~(b). The labels 1 through 12 designate January through December of each year. The significance interval at 1 % level is roughly the size of each symbol in the lower panel.

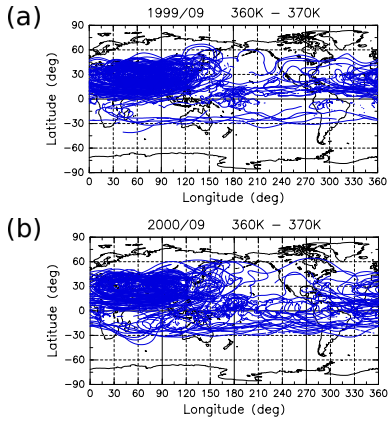

Figure 4. Horizontal projection of the backward trajectories extracted within the potential temperature levels between 360 and 370 K. The initialization is made on 400 K potential temperature surface between 30° N and S from the equator (Sect. 2) in (~~top~~a) September 1999 and (~~bottom~~b) September 2000. The illustration is limited to the subset of trajectories as in Fig. 1 for visual clarity.

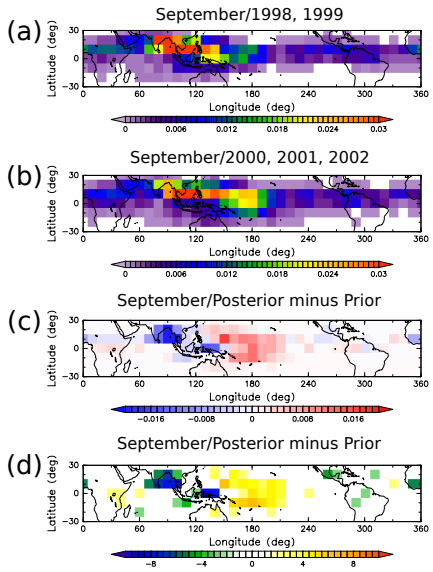

Figure 5. ~~Horizontal distribution of LCP-event probability estimated from~~ Horizontal distribution of LCP-event probability, $P(\mathrm{LCP} \in j)$, estimated from the TST trajectories initialized on 400 K ~~in (top) September~~ in (a) September 1998 and 1999 ~~(prior to the drop) and (second from the top) September~~ (prior to the drop) and (b) September 2000, 2001 and 2002 ~~(posterior to the drop). The probabilities are estimated in~~ (posterior to the drop). The probabilities are estimated in 10° by 10° longitude–latitude ~~bin as the number of LCPs experienced by all TST air parcels inside the bin divided by the total number of TST parcels used for the calculation. The difference of probabilities between the two (posterior minus prior to the drop) and the values of test statistic transformed to the standard Gaussian distribution are shown in the third and the bottom panel, respectively. The test statistic is derived from the difference of the ratio of LCP occurrences assuming binomial distribution for the two populations. The colored bins indicate that the difference is statistically significant at the significance level of~~ bin as the number of LCPs experienced by all TST air parcels inside the bin divided by the total number of TST parcels used for the calculation ($N(\mathrm{LCP} \in j)/N_{\mathrm{TST}}$). Panels (c) and (d) are the difference of probabilities between the two (posterior minus prior to the drop) and the values of test statistic (T_1 of Appendix A1), respectively. The colored bins indicate that the difference is statistically significant at the significance level of 1 % ~~or higher. Those bins shown in white indicate there found no LCP event in the top two panels, while the difference is not statistically significant in the bottom two.~~or higher. Those bins shown in white indicate there found no LCP event in (a) and (b), while the difference is not statistically significant in (c) and (d). See Appendix for the details of statistical tests.

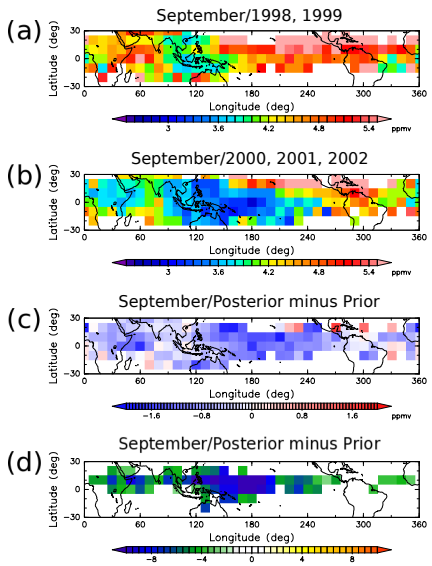

Figure 6. ~~The same as Fig. 5 except that the ensemble mean values of SMR_{min} are illustrated on the bin-by-bin basis. The test statistic~~ is t values derived from the difference of sample means.

The same as Fig. 5 except that the ensemble mean values of SMR_{min} are illustrated on the bin-by-bin basis (SMR(LCP$\in j$)). The test statistic shown in (d) is T_2 of Appendix A2. See Appendix for the details.

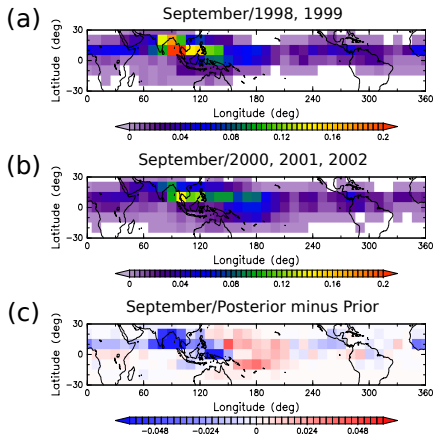

Figure 7. The same as the top three panels of Fig. A2 ~~except that the contribution of each bin to the $_e$ (ppmv) is illustrated. The value for each bin is the expectation value as calculated~~ by ~~multiplying~~ the ~~probability (Fig. 5) by the~~ ensemble mean $\mathrm{SMR}_{\mathrm{min}}$ (Fig. A2).

except that $E(\mathrm{LCP} \in j)$, the contribution of bin j to $[\mathrm{H_2O}]_e$, (ppmv) is illustrated. See text for the definition of $E(\mathrm{LCP} \in j)$.

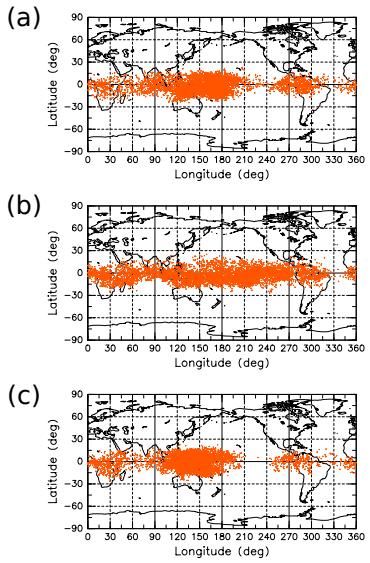

Figure 8. Horizontal distribution of LCP taken by all TST trajectories initialized on 400 K isentrope in February (top) 1997, (middle) 1998, and (bottom) 1999.

in February (a) 1997, (b) 1998, and (c) 1999.

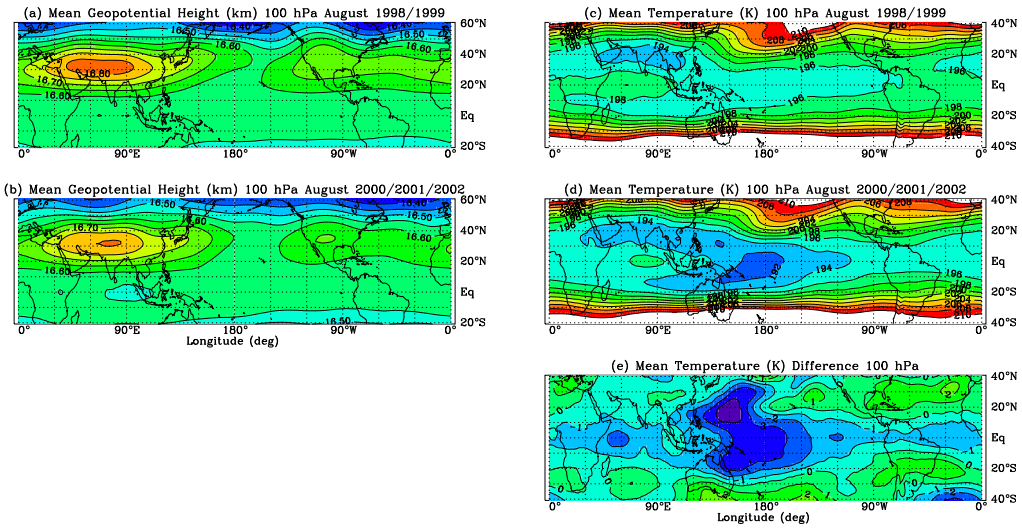

Figure 9. Longitude-latitude sections of (left) geopotential height (km) and (right) temperature (K) on 100 hPa averaged in August 1998 and 1999 (~~top~~a, c) and 2000, 2001 and 2002 (~~middle~~b, d) and the difference between the two (~~bottom~~e) estimated from ERA Interim dataset. Note the difference of latitudinal range between the left and the right side figures.

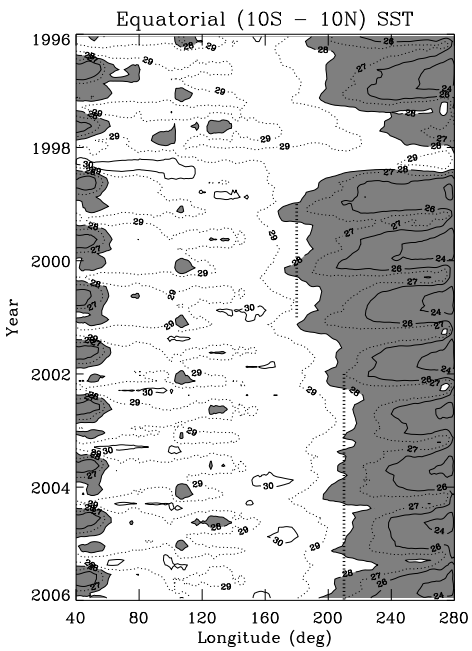

Figure 10. Longitude-time section of sea surface temperature (SST) averaged over the oceanic region of the latitude band between 10° N and S of the equator during the period from January 1996 to December 2005. The region with the SST colder than 28 °C is shaded. The dashed line spans from January 1999 to December 2000 along 180° E and from January 2002 to December 2006 along 210° E. Data are from NOAA OI SST V2.

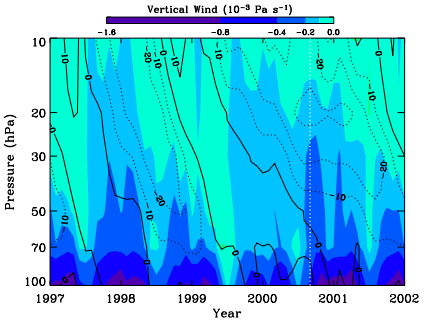

Figure 11. Time-height section of the zonally and latitudinally (within 15° N and S) averaged monthly mean vertical (color; 10^{-3} Pa s^{-1}) and zonal (contour; m s^{-1}) wind velocities from January 1997 to December 2001 calculated from ERA Interim dataset. Solid (dashed) contours are westerlies (easterlies). Tick marks are January of the corresponding year, and the vertical dashed line in white marks September 2000.

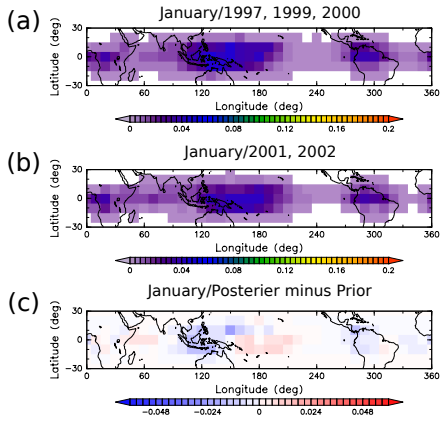

Figure 12. The same as Fig. A2 but for January. Those values in 1997, 1999, and 2000 are used for the calculations prior to the drop, while 2001 and 2002 are used for the posterior. Those in January 1998 are not used due to the influence of El Niño (see text).

ACPD

Manuscript prepared for Atmos. Chem. Phys.
with version 2015/04/24 7.83 Copernicus papers of the LaTeX class copernicus.cls.
Date: 18 December 2015

A Lagrangian description on the troposphere-to-stratosphere transport changes associated with the stratospheric water drop around the year 2000

F. Hasebe[1,2] and T. Noguchi[2,a]

[1]Faculty of Environmental Earth Science, Hokkaido University, Sapporo, Japan
[2]Graduate School of Environmental Science, Hokkaido University, Sapporo, Japan
[a]now at: Human Asset Management and Corporate Affairs Unit, FUJITSU FSAS INC., Kawasaki, Japan

Correspondence to: F. Hasebe (f-hasebe@ees.hokudai.ac.jp)

Abstract. Stratospheric water vapor is known to have decreased suddenly at around the year 2000 to 2001 after a prolonged increase through the 1980s and 1990s. This stepwise change is studied by examining the entry value of water to the stratosphere ($[H_2O]_e$) and some Lagrangian diagnostics of dehydration taking place in the Tropical Tropopause Layer (TTL). The analysis is made using the backward kinematic trajectories initialized every $\sim$ 10 days since January 1997 till December 2002 on 400 K potential temperature surface in the tropics. The $[H_2O]_e$ is estimated by the ensemble mean value of the water saturation mixing ratio (SMR) at the Lagrangian cold point (LCP) where SMR takes minimum (SMR_{min}) in the TTL before reaching the 400 K surface. The drop in $[H_2O]_e$ is identified to have occurred in September 2000. The horizontal projection of September trajectories, tightly trapped by anticyclonic circulation around Tibetan high, shows eastward expansion since the year 2000. Associated changes are measured by three-dimensional bins, each having the dimension of 10° longitude by 10° latitude within the TTL. The probability distribution of LCPs shows appreciable change exhibiting a composite pattern of two components: (i) the dipole structure consisting of the decrease over the Bay of Bengal and Malay Peninsula and the increase over the northern subtropical western Pacific and (ii) the decrease over the equatorial western Pacific and the increase over the central Pacific almost symmetric with respect to the equator. The SMR_{min} shows general decrease in the tropics with some enhancement in the central Pacific. The expectation values, defined by the multiple of the probability of LCP events and the ensemble mean values of SMR_{min}, are calculated on each bin for both periods prior and posterior to the drop. These values are the spatial projection of $[H_2O]_e$ on individual bin. The results indicate that the drop is brought about by the decrease of water transport borne by the air parcels having experienced the LCP over the Bay of Bengal and the western tropical Pacific. The former is related to the eastward expansion of the anticyclonic circulation around the weakened Tibetan high, while the latter will be linked to the eastward

expansion of western tropical warm water to the central Pacific. This oceanic surface forcing may be responsible also for the modulation of dehydration efficiency in the successive northern winter. The drop in September 2000 and the sustained low values thereafter of $[H_2O]_e$ are thus interpreted as being driven by the changes in thermal forcing from the continental and oceanic bottom boundaries.

1 Introduction

Stratospheric water vapor (SWV) observed by balloon-borne hygrometers exhibits gradual increase in the 1980s and 1990s (Oltmans and Hofmann, 1995; Oltmans et al., 2000) followed by a stepwise drop at around the year 2000 (Scherer et al., 2008; Fujiwara et al., 2010). Since SWV has a positive radiative forcing as a greenhouse gas (Shindell, 2001), its possible increase during the two decades could have caused enhanced surface warming by about 30 % as compared to that without taking this increase into account, while the subsequent drop could have slowed down the surface warming by about 25 % from about 0.14 to 0.10 °C per decade (Solomon et al., 2010). The cause and mechanism of this stepwise change have been fluently discussed (e.g., Randel et al., 2006; Rosenlof and Reid, 2008; Bönisch et al., 2011; Fueglistaler, 2012; Fueglistaler et al., 2014; Dessler et al., 2014). While constructing a reliable long-term SWV record is still a challenge (Hegglin et al., 2014), the understanding of a possible stepwise change in SWV is required in assessing possible modulation of the Brewer–Dobson circulation under global warming.

The variation of SWV is driven dynamically by the troposphere-to-stratosphere transport of water and chemically by the oxidation of methane. The dynamical control is mostly associated with the efficiency of dehydration functioning on the air mass advected in the TTL (Holton and Gettelman, 2001; Hatsushika and Yamazaki, 2003). The reproduction of SWV variations by using the Lagrangian temperature history along the trajectories (e.g., Fueglistaler et al., 2005; Dessler et al., 2014) has proven quite effective, even though the quantitative estimation of the water amount entering the stratosphere requires detailed consideration dealing with aerosols and ice particles (ice nucleation and sublimation processes, supersaturation, and deposition and precipitation of ice particles) as well as the minute description of meteorological conditions (subgrid-scale variabilities, intrusion of deep convection into advected air parcels, and irreversible mixing due to breaking waves along with the ambiguity in the analysis field).

Here, we discuss the cause of the stepwise drop in SWV by making the analysis of the entry mixing ratio of water to the stratosphere ($[H_2O]_e$) with the aid of some Lagrangian diagnostics of TTL dehydration such as the preferred advection pathways in the TTL, the location in which water saturation mixing ratio (SMR) takes minimum along each trajectory (Lagrangian cold point; LCP) together with its occasional value (SMR_{min}) before entering the stratosphere (Sect. 3). The backward kinematic trajectories initialized on 400 K potential temperature surface in the tropics, similar to those of Fueglistaler et al. (2005), are used. The calculations cover the period from January 1997

to December 2002. The statistical features of the LCP and SMR_{min} are analyzed for the 90 day trajectories in which the air parcels experienced LCP in the TTL (Sect. 2). The analysis is focused on the examination of the entry value of water to the stratosphere, meaning that any contribution from the recirculation within the stratosphere (ST) and the sideway entry of water to ST without taking the LCP in the TTL are intentionally left out of the scope. Detailed examinations on the driving mechanism itself are left for future studies. However, it will reveal the direct cause that may have led to the SWV drop in Lagrangian framework. This approach has the advantages over Eulerian description because the drop in SWV does not necessarily mean TTL cooling conveniently described in Eulerian framework. For example, it might simply reflect the change in the proportion of air parcels that have passed the coldest region in the TTL. Conversely, any extreme cooling does not necessarily result in enhanced dehydration as long as the air parcels do not experience LCP event in that region. We will try to describe a hypothetical story on the cause of the stepwise drop of SWV through the discussion of the results in Sect. 4. Conclusions are placed in Sect. 5.

2 Method of analysis

2.1 Trajectory calculations

The method of estimating $[H_2O]_c$ in the present study is similar to that of Fueglistaler et al. (2005). $[H_2O]_e$ at time t is estimated as the ensemble mean value of SMR_{min} along 90 day backward kinematic trajectories initialized at t. The trajectory calculations are started from uniformly distributed gridpoints (every 5.0° longitude by 1.5° latitude) within 30° N and S from the equator on 400 K potential temperature surface, which results in 2952 initialization points in total for a single calculation. The calculations are started from the 5th, 15th, and 25th of every month during the period since January 1997 till December 2002 relying on the European Centre For Medium-Range Weather Forecasts ERA Interim dataset (Dee et al., 2011). All meteorological variables on the 60-layer model levels have been converted to those on pressure levels keeping the horizontal resolution of 0.75° by 0.75° longitude–latitude gridpoints prior to calculations.

2.2 Selection of trajectories relevant to TTL dehydration

The meridional projections of the backward trajectories extracted from those initialized on 15 January 1999 are shown in Fig. 1. The top and bottom diagrams are the same except that pressure (top) and potential temperature (bottom) are taken as the ordinate. The asterisks in red indicate the location of the LCP while those in green are the termination point of trajectory calculations (90 days before initialization at the longest). In case the backward extension of the trajectories hit the surface of the earth, the calculations are terminated at that point, and those portions of the trajectories immediately before the surface collision are used for the analysis. The migration of air parcels depicted in the trajectories is roughly categorized into three major branches: quasi-isentropic advection in

the TTL and the lower stratosphere (LS), vertical displacement in the troposphere due to diabatic motion resolvable in grid-scale velocity field, and quasi-isentropic migration in the troposphere. We can see many air parcels are traced back to the troposphere representing the tropical troposphere-to-stratosphere transport (TST), while some portion of the trajectories remain in the LS and/or reach the tropical 400 K surface by taking the sideways without making excursions in the TTL. All non-TST trajectories are removed from the following analysis to focus our discussion on the modulation of $[H_2O]_e$. For the sake of clarity, the TST particles in the present study are defined as a subset of those particles traceable down to 340 K having recorded LCP in the TTL. For the application of this LCP condition to our trajectories, we introduce the Lagrangian definition of the TTL to assure internal consistency of the analysis.

The motion of air parcels ascending in the tropical troposphere is characterized by rapid convective up-lift that accompanies latitudinal migration associated with the seasonal displacement of the Inter-Tropical Convergence Zone. Up in the TTL, on the other hand, the diabatic ascent is driven by radiative heating, in which the seasonal migration with respect to latitude is much smaller than that in the troposphere because the dynamical field generated by the thermal forcing at the bottom boundary retains relatively high symmetry with respect to the equator. By translating these features into the characteristics of trajectories, we derive a definition of the TTL in a Lagrangian fashion.

Figure 2 on the top illustrates the vertical distribution of the proportion of trajectories categorized on a daily basis as "fast" ascending air parcels. The required rate for the fast ascent is set to more than 0.2 K in potential temperature within 1 time step (30 min), that is, the condition for θ K isentrope is met if the air parcel crosses θ K surface from below $\theta - 0.1$ K to above $\theta + 0.1$ K in 30 min. We can see that the proportion of the fast diabatic ascent thus defined takes maximum at around 340 K in the troposphere and minimum at around 355 K. The proportion of such "fast" air parcels reduces above the level of main outflow and rapidly decays toward the level of zero net radiative heating in the TTL. Above this level, the air parcels are diabatically lifted up by radiative heating and further pumped-up by dissipating planetary waves in the midlatitude stratosphere (Holton et al., 1995). The alternation of the primary forcing that drives diabatic ascent is also seen from the bottom panel of Fig. 2, which shows the seasonal migration of the latitudinal position of the trajectories traceable to down below 340 K averaged for (blue) January, (green) April, (yellow) July, and (red) October. The altitude of the kink at around 355 K suggests that the influence of tropical convective motion almost ceases at this level and the diabatic forcing gradually shifts to radiative heating in the TTL and above.

The diagnostic features depicted in Fig. 2 agree that the bottom of the TTL would be most properly defined at 355 K potential temperature level for our study. In the following analysis, we make use of TST trajectories defined by the air parcels that have ascended from the lower troposphere below 340 K isentrope experiencing the LCP in the TTL, which is defined by the layer between the isentropic levels 355 and 400 K within 30° N and S from the equator.

3 Results

3.1 The drop in $[H_2O]_e$

The evolution of the entry value of water to the stratosphere as modeled in $[H_2O]_e$ time series is shown in Fig. 3. The top panel is the sequential change in the monthly ensemble mean value of $[H_2O]_e$ estimated from the TST air parcels during the period between January 1997 and December 2002. We can see the decrease of the seasonal maxima in boreal summer in 2000. The seasonal minima in boreal winter, on the other hand, show larger values in January–February 2000 as compared to those in 1999, 2001, and 2002 and thus the drop in $[H_2O]_e$ is not quite obvious. As the six-year time series is not long enough to define climatology and anomalies from it, we simply view the interannual variations on the basis of each calendar month. The bottom panel of Fig. 3 is the same as the top except that the data points are connected by each calendar month. When viewed in this way, the drop in the year 2000 of about 1 ppmv shows up in the time change in September (marked by 9), October (10), November (11), and December (12). Similar drop continues to January (1) and the successive months in 2001. As there is little difference between those in August 1999 and 2000, we may well conclude that the drop in $[H_2O]_e$ occurred in September 2000. Considering the time period required for the air parcels to make excursion in the TTL, we may interpret that the change in the characteristics of dehydration has been initiated in the boreal summer of 2000. The maxima of $[H_2O]_e$ in January through June 1998 are related to the strong El Niño as is discussed later in Sect. 4.

3.2 Horizontal projection of the TST trajectories

As the first step of examining the change in the characteristics of TTL dehydration initiated in northern summer of 2000, Fig. 4 illustrates the horizontal projection of TST trajectories within the layer between the isentropes 360 and 370 K extracted from those initialized in September 1999 (top) and 2000 (bottom). In spite of the equatorially symmetric assignment of the initialization points on 400 K potential temperature surface, the trajectories in the TTL are highly asymmetric with respect to the equator and clustered mostly in the northern subtropics. The dense population of the trajectories shows that the air parcels are largely trapped by Tibetan high in the region between 30° W to 150° E and 0 to 45° N. Comparison between the two, representing September trajectories prior and posterior to the drop, respectively, reveals that the circulation of air parcels around the Tibetan high is loosely tied to the center in the latter period, resulting in the expansion of the anticyclonic circulation branch mostly to the east accompanied by the spread-out of the trajectories farther to the Southern Hemisphere in the latter. This modal shift in the trajectories initialized in September occurs in the year 2000 and continues at least through 2001 and 2002 (not shown).

3.3 Statistical distribution of the LCP

The shift in the circulation pattern of air parcels is not enough to characterize the modification of dehydration efficiency in the TTL. Randel and Jensen (2013) discuss the monsoon circulation during boreal summer in the context of the influence of northern midlatitude on the TTL. The horizontal structure of ozone and water vapor on 390 K potential temperature surface (Randel and Jensen, 2013, Figs. 2 and 4) suggests an intrusion of the ozone-rich midlatitude air into the TTL possibly contributing to the TTL hydration during boreal summer. For the purpose of identifying the change in the dehydration efficiency associated with the modal shift seen in Fig. 4, the numbers of LCPs are counted by every 10° longitude-latitude bin in the tropics. The probabilities of LCPs are estimated for each bin by dividing the LCP counts by the total number of TST trajectories. The top two panels of Fig. 5 show the horizontal distributions of the probabilities of LCP events thus obtained for those trajectories initialized in September 1998 and 1999 (top; prior to the drop) and September 2000, 2001 and 2002 (second panel; posterior to the drop). The spatial maximum during the period prior to the drop is found over the Bay of Bengal and Malay Peninsula with the ridge extending to South China Sea (top). During the period posterior to the drop (second panel), this maximum shows eastward expansion as far as 150° E. There also appears some increase in the Central Pacific covering both northern and southern subtropics crossing over the equator. These two components appear clearer in the difference field shown in the third panel. Those bins shown in blue (red) indicate the decrease (increase) of the LCP probabilities in the posterior period. The test statistic of the difference transformed to the standard Gaussian distribution is shown in the bottom panel of the figure indicating the region in which the differences are statistically significant at the significance level of 1 % or higher. It is interesting to note that, in addition to the dipole structure associated with the eastward expansion of the Tibetan anticyclone, the probabilities show significant decrease over the equator at around 130 to 140° E and increase in wider area almost symmetric with respect to the equator (160° E to 160° W and 10° S to 10° N). This structure will be discussed further in Sect. 4.

3.4 Statistical change in the SMR_{min}

The increase of the LCP events in some bins does not necessarily mean enhanced dehydration over there. The next step is to examine the change in the SMR_{min}. Simultaneous with counting the LCP events, the values of SMR at the time of each LCP event (SMR_{min}) have been summed-up to calculate the average for each bin. Figure 6 is the same as Fig. 5 except that the ensemble mean SMR_{min} are illustrated rather than the probability of LCP events. We can see that the averages of SMR_{min} in the tropics are roughly smaller in the eastern than in the western hemisphere accompanying a broad minimum of about 3.5 to 3.7 ppmv over the maritime continent during the period prior to the drop (top). The values show general decrease in the tropics with some enhanced drop in the central Pacific reaching less than 3.0 ppmv in the period posterior to the drop (second panel from the top),

leading to a reversal of zonal gradient of SMR_{min} over the equator. The difference between the two (third panel), together with the statistical significance (bottom), confirms the pronounced decrease of SMR_{min} in the central Pacific after 2000. On the other hand, the change of SMR_{min} associated with the east-west dipole structure is not so remarkable in terms of the difference of SMR_{min}, although the tendency is the same.

3.5 Statistical change in the expectation values

While the differences of SMR_{min} appear smaller over the Bay of Bengal and Malay Peninsula than over the central Pacific, the comparisons based only on the changes in SMR_{min} could be misleading, because the probabilities of LCP events are much higher in the former than in the latter (Fig. 5). Figure 7 shows the horizontal distribution of the expectation value of $[H_2O]_e$ estimated by multiplying the probability of LCP events (Fig. 5) and the ensemble mean SMR_{min} (Fig. 6) together for each bin. This corresponds to the projection of $[H_2O]_e$ onto each bin. We can see that the September values of $[H_2O]_e$ are mostly projected to the Bay of Bengal and Malay Peninsula before the drop (top panel). The contribution from this core area remains dominant during the posterior period (middle panel). The reductions (bottom panel) are mainly due to the decreases of the LCP-event probability (Fig. 5) cooperated by the reduced ensemble mean SMR_{min} (Fig. 6). The corresponding increase of LCP-event probabilities especially that over the central Pacific has contributed to a slight increase in $[H_2O]_e$ because the magnitude of increase in occurrence frequency prevails that of the decrease in SMR_{min}. The resultant changes could be interpreted as the composite of two components: (i) the decrease over the Bay of Bengal and (ii) the decrease over the equatorial western Pacific and the increase over the central Pacific almost symmetric with respect to the equator extending to the subtropical latitudes of both hemispheres. The former is supplemented by slight decrease widespread along the 10° N zonal belt with the exception around 150° E and the central Pacific. These features will be related to the eastward expansion of the anticyclonic circulation around the Tibetan high, while the latter is suggestive of some response to the thermal forcing from the equatorial ocean.

4 Discussion

4.1 Maxima of $[H_2O]_e$ in 1998

We have seen in Fig. 3 that the time series of $[H_2O]_e$ shows maxima in January through June 1998. We excluded these months from our analysis in Sect. 3 because of the influences of strong El Niño. The values of $[H_2O]_e$ in November and December 1997 are larger than those in 1998, which may suggest possible influence of El Niño also in these months. The reason why we regard these facts as little related to the drop of $[H_2O]_e$ in 2000 is briefly discussed here.

For exploration of the reason of such anomalies, the horizontal distributions of LCP are shown for those initialized in February 1997, 1998 and 1999 in Fig. 8. The distributions in February 2000, 2001

and 2002 (not shown) are similar to those of 1997 and 1999. The LCPs in February are commonly distributed almost symmetric with respect to the equator, but the longitudinal distribution is not uniform. High concentration in the western tropical Pacific in 1997 and 1999 (and also in 2000, 2001 and 2002) is suggestive of the strong influence of the warm sea surface temperature (SST) on the LCP distribution. The large scatter extending to the eastern tropical Pacific in 1998 is due to the migration of the large scale convective system to the east associated with the strong El Niño. We have put this anomalous change out of the scope of the present study, because those anomalous values seem to have recovered to normal by the northern summer of 1998 (well before 2000) and there is no reasoning that this strong El Niño is coupled to the drop in $[H_2O]_e$ in 2000. For the objective judgement of the influence of the El Niño, we employ the SST averaged in the region between 90° W and 150° W longitude and 5° S to 5° N latitude (Niño 3 region, Trenberth, 1997). Those months exhibiting the SST anomalies (relative to the 1981-to-2010 climatology) greater than 1.5 times the standard deviation are excluded from the present analysis. Those excluded are the twelve months from June 1997 to May 1998.

4.2 Perspective to the mechanism of the drop

The entry value of water to the stratosphere, $[H_2O]_e$, estimated by the ensemble mean values of SMR_{min} along the TST trajectories shows appreciable decrease in September 2000 (Fig. 3), suggesting some modulation in the dehydration efficiency functioning on the air parcels advected in the TTL during the northern summer of 2000. The horizontal projection of trajectories initialized in September, characterized by anticyclonic circulation associated with Tibetan high in the TTL, shows eastward expansion in the year 2000 accompanied by some bifurcation to the Southern Hemisphere (Fig. 4). This modal shift appears as decreases in the probability distribution of the LCP over the Bay of Bengal and the western tropical Pacific (Fig. 5). The SMR averaged on the occasion of LCP events (SMR_{min}) shows general decrease with some enhancement in the central Pacific (Fig. 6). These results suggest two possible components contributing to the sudden drop of $[H_2O]_e$ in September 2000: the modulations of the Tibetan high and the thermal forcing from the equatorial ocean. The contribution from these two components has been quantified by projecting the $[H_2O]_e$ onto bins distributed in the tropics (Fig. 7). The results indicate that the drop is brought about by a response of the TTL circulation to the modulated forcing both from the continental summer monsoon and the equatorial ocean. It is thus quite interesting to take a brief look at the changes in the TTL meteorological fields in Eulerian framework before concluding this study.

Figure 9 illustrates the longitude-latitude section of 100 hPa geopotential height (left) and temperature (right) averaged in August 1998 and 1999 (top) and 2000, 2001 and 2002 (middle). These are the background Eulerian fields having roughly brought about the Lagrangian features described by the top two panels of Figs. 5–7. The corresponding features appear basically the same if we look at individual August without taking the average. We can see the Tibetan anticyclone in the height

field of both periods (left) with the intensity weaker in the latter (2000/2001/2002). The expansion of the trajectories after 2000 (Fig. 4), therefore, is the result of loosened grip of air parcels around weakened Tibetan high in the latter years. These features remain the same in September of other years posterior to the drop (not shown). The temperature field (right-hand side) both prior and posterior to the drop appears as the typical pattern of the TTL response to the thermal forcing at the bottom boundary with additional heating to the subtropical Northern Hemisphere (Matsuno, 1966; Gill, 1980). The difference (bottom panel) indicates substantial cooling in the northern subtropics at around 150° E and the central Pacific. The latter corresponds to the findings of Rosenlof and Reid (2008) in which the tropical tropopause temperature in 171 to 200° E longitude band decreased in association with the SWV drop in 2000.

The correspondence of the decrease of the equatorial 100 hPa temperature to the increase of the underlying SST is explored in Fig. 10, which shows the longitude-time section of the equatorial SST averaged between 10° N and S of the equator. We could see the warm SST region in the western Pacific expands to the east in the year 2000, and the contour of 28 °C, the threshold of active convection (Gadgil et al., 1984), during the coldest month of the year crossed the date line in 2001. The difference between the longitudes of warm SST core and the temperature minimum near the tropopause, noticed already by Rosenlof and Reid (2008), is due to the eastward tilt of cold region associated with a steady Kelvin wave response to underlying convective heating (Hatsushika and Yamazaki, 2003). The warm condition in the central Pacific continues at least till the end of 2005. The decrease of 100 hPa temperature over the central Pacific is, thus, well correlated to this SST variation. The important point in our analysis is that the drop of $[H_2O]_c$ does not come from the decrease of TTL temperature in the central Pacific but that from the water transport by way of the Bay of Bengal and the western tropical Pacific (Fig. 7).

The study by Young et al. (2012), discussing the changes in the Brewer–Dobson circulation during the period 1979 to 2005 by referring to the out-of-phase temperature relationship between the tropics and the extratropics, found no appreciable change around the year 2000. However, the zonally uniform component exhibiting the out-of-phase relationship between the tropics and the extratropics in 100 hPa temperature difference (Fig. 9) is suggestive of some stratospheric contribution to the drop in $[H_2O]_c$ (Randel et al., 2006) through wave-driven pumping (Holton et al., 1995). Actually the analysis of dynamical fields such as eddy heat flux and EP-flux by Fueglistaler (2012) finds a strengthening of the residual circulation qualitatively consistent with the drop of SWV in *October* 2000. Figure 11 shows in color the time-height section of monthly mean vertical wind velocity in the tropics. The seasonal enhancement in the upward motion during northern winter shows up in the lowermost stratosphere. The solid and dashed contours superposed on the vertical velocity field are the zonal wind components depicting the westerly and the easterly phase, respectively, of the quasi-biennial oscillation (QBO). The stagnation of the downward propagation specifically that of the easterly phase of the QBO is noticed in late 1997 to early 1998 and late 2000 to early 2001 at

around 40 hPa level. This phase dependency of the stagnant propagation is brought about by the secondary circulation of the QBO in which the upward (downward) motion accompanies the easterly (westerly) shear zone of the QBO (Plumb and Bell, 1982; Hasebe, 1994). What is interesting here is that the enhanced upward motion is found in September and October 2000 blocking the downward propagation of easterlies. The limitation from our use of Eulerian vertical velocity, rather than TEM residual velocity, will be minimal as we focus our discussion in the tropics. Actually the anomalies in the equatorial upwelling at 78 hPa estimated by Rosenlof and Reid (2008) show similar results. Further analysis by Fueglistaler et al. (2014) emphasize that the strengthening of the residual circulation does not last long but continues for a few years around the year 2000. Remembering the time of excursion for air parcels circulating the Tibetan high (Fig. 4), the stratospheric anomalies in October 2000 (Fueglistaler, 2012) appears later than the initiation of the drop in $[H_2O]_e$. The difference of one month, albeit small, is large enough to be resolved in the analysis. Then the enhanced upwelling discussed by Fueglistaler et al. (2014) might be the stratospheric response to the tropospheric forcing that modulated the dehydration efficiency in the preceding boreal summer of 2000 rather than the direct cause of the SWV drop. Further studies employing numerical simulations are definitely required. It is worth mentioning here that the enhancement of the Brewer–Dobson circulation may have occurred also in the northern hemispheric branch; the age of northern mid-latitude stratospheric air diagnosed by the CO_2 concentration appears shorter than usual in 2002 (Engel et al., 2009, Fig. 3), although the difference is not statistically significant.

4.3 Perspective to the mechanism of sustained low amount of $[H_2O]_e$

We have seen some background meteorological fields from Eulerian perspective to interpret the evidences presumably responsible for the drop of $[H_2O]_e$ in September 2000 described in Lagrangian framework. The problems not yet answered are what is the specific event (if any) and how is it generated that has triggered the sequence of phenomena that ultimately led to the sudden drop of SWV. In addition, the sustained low values of $[H_2O]_e$ after September 2000 need some mechanism that lasts longer than the seasonal time scale, since the modulation of Tibetan high cannot explain the reduction continuing to the successive months in northern winter (Fig. 3).

Figure 12 is the same as Fig. 7 except that the January projection is illustrated. We can see, in addition to the values generally lower than those in September, the larger values are found in the western tropical Pacific (top and middle panels), indicating the January values of $[H_2O]_e$ are controlled by those over the western Pacific. This is consistent with the picture having been presented in numerical simulations (Hatsushika and Yamazaki, 2003). The difference between the two periods (the bottom diagram) shows decrease over Indonesia and increase over the central Pacific during the period posterior to the drop. This pattern in January is brought about by the combination of the decrease (increase) of LCP-probability and the slight (enhanced) decrease of SMR_{min} values over the western (central) Pacific (not shown). These evidences suggest that the drop of $[H_2O]_e$ in

northern winter is due to the response of the TTL circulation to the eastward expansion of the warm water to the central Pacific (Fig. 10).

The correspondence to the change in the SST distribution, the time of occurrence, and the persistency of phenomenon suggest that the drop and the subsequent low values of $[H_2O]_e$ are brought about by the eastward expansion of warm SST region to the central Pacific through reduced water entry to the stratosphere. Then our hypothetical story may read, the eastward expansion of warm SST region brings about the reduction of $[H_2O]_e$ by TST air parcels passing through the western tropical Pacific during northern winter (Fig. 12), while the heating from the modulated SST mentioned above, competing against that over the continent, has led to the modal shift of trajectories during northern summer resulting in the reduced water transport over the Bay of Bengal and the western tropical Pacific (Fig. 7).

The above speculation might end up with some proper explanation on the cause of the eastward expansion of the equatorial warm water to the central Pacific observed in 2000. In this context, it is interesting to see possible occurrence of "El Niño Modoki" characterized by the warm SST event over the central Pacific (W. J. Randel, personal communication, 2015). Actually the time series of normalized ENSO Modoki index of Ashok et al. (2007) turns from prolonged negative to positive towards 2001. It is also interesting to note that the "La Niña-like condition," tied to the surface cooling of the equatorial eastern Pacific, is supposedly responsible for the recent hiatus, the pause of the global-mean surface air temperature rise through the strengthening of ocean heat uptake (Kosaka and Xie, 2013; Watanabe et al., 2014). If proved to be true, we may have unveiled another piece of pathways the internal variability of our climate system could exert on the surface cooling through SST-driven SWV fluctuations.

5 Conclusions

Backward kinematic trajectories, initialized on 400 K potential temperature surface in the tropics, have been employed to describe the stratospheric water drop observed at around 2000 to 2001 from a Lagrangian point of view. The entry value of water to the stratosphere, $[H_2O]_e$, shows appreciable decrease in the trajectories initialized in September 2000 suggesting the change in the TTL dehydration efficiency during the boreal summer of 2000. The following changes are found to be responsible for the drop in $[H_2O]_e$. The reduction of water vapor transported by those air parcels that experienced LCP events in two regions; over the Bay of Bengal and the western tropical Pacific. The reductions are brought about by the decreases in both the LCP-event probability and the ensemble mean SMR_{min} over there. The LCP reduction in the former region is related to the modified migration pathways of air parcels circulating the weakened Tibetan anticyclone, while that in the latter may be a response to eastward expansion of warm water to the central Pacific. This SST modulation seems to be responsible also for the decrease of $[H_2O]_e$ in the successive northern winter. Some

indication of stratospheric contribution through intensified pumping appears only intermittent and will be better interpreted as a response to tropospheric forcing changes.

Acknowledgements. This work is based on the Master of Science Thesis of T. Noguchi submitted to the Graduate School of Environmental Science, Hokkaido University in February 2015. T. Noguchi is grateful to the members of the Graduate School of Environmental Science for the encouragement and discussions through the preparation of his thesis. The discussion with Koji Yamazaki of Hokkaido University is greatly appreciated. The results in part have been presented at the CT3LS Meeting having been held in July 2015. F. Hasebe is grateful to the comments from meeting participants especially W. J. Randel of NCAR and K. H. Rosenlof of NOAA. NOAA OI SST V2 data are provided by the NOAA/OAR/ESRL PSD, Boulder, Colorado, USA, from their Web site at http://www.esrl.noaa.gov/psd/. This work was supported by the Japan Society for the Promotion of Science, Grant-in-Aid for Scientific Research (S) 26220101.

Revised

Manuscript prepared for Atmos. Chem. Phys.
with version 2015/04/24 7.83 Copernicus papers of the LaTeX class copernicus.cls.
Date: 18 December 2015

A Lagrangian description on the troposphere-to-stratosphere transport changes associated with the stratospheric water drop around the year 2000

F. Hasebe[1,2] and T. Noguchi[2,a]

[1]Faculty of Environmental Earth Science, Hokkaido University, Sapporo, Japan
[2]Graduate School of Environmental Science, Hokkaido University, Sapporo, Japan
[a]now at: Human Asset Management and Corporate Affairs Unit, FUJITSU FSAS INC., Kawasaki, Japan

Correspondence to: F. Hasebe (f-hasebe@ees.hokudai.ac.jp)

Abstract. The sudden decrease of stratospheric water vapor at around the year 2000 to 2001 is relatively well accepted in spite of the difficulty to quantify the long-term variations. This stepwise change is studied by examining the entry value of water to the stratosphere ($[H_2O]_e$) and some Lagrangian diagnostics of dehydration taking place in the Tropical Tropopause Layer (TTL). The analysis is made using the backward kinematic trajectories initialized every $\sim$ 10 days since January 1997 till December 2002 on 400 K potential temperature surface in the tropics. The $[H_2O]_e$ is estimated by the ensemble mean value of the water saturation mixing ratio (SMR) at the Lagrangian cold point (LCP) where SMR takes minimum (SMR_{min}) in the TTL before reaching the 400 K surface. The drop in $[H_2O]_e$ is identified to have occurred in September 2000. The horizontal projection of September trajectories, tightly trapped by anticyclonic circulation around Tibetan high, shows eastward expansion since the year 2000. Associated changes are measured by three-dimensional bins, each having the dimension of 10° longitude by 10° latitude within the TTL. The probability distribution of LCPs shows appreciable change exhibiting a composite pattern of two components: (i) the dipole structure consisting of the decrease over the Bay of Bengal and Malay Peninsula and the increase over the northern subtropical western Pacific and (ii) the decrease over the equatorial western Pacific and the increase over the central Pacific almost symmetric with respect to the equator. The SMR_{min} shows general decrease in the tropics with some enhancement in the central Pacific. The expectation values, defined by the multiple of the probability of LCP events and the ensemble mean values of SMR_{min}, are calculated on each bin for both periods prior and posterior to the drop. These values are the spatial projection of $[H_2O]_e$ on individual bin. The results indicate that the drop is brought about by the decrease of water transport borne by the air parcels having experienced the LCP over the Bay of Bengal and the western tropical Pacific. The former is related to the eastward expansion of the anticyclonic circulation around the weakened Tibetan high, while the latter

will be linked to the eastward expansion of western tropical warm water to the central Pacific. This oceanic surface forcing may be responsible also for the modulation of dehydration efficiency in the successive northern winter. The drop in September 2000 and the sustained low values thereafter of $[H_2O]_e$ are thus interpreted as being driven by the changes in thermal forcing from the continental and oceanic bottom boundaries.

1 Introduction

Stratospheric water vapor (SWV) observed by balloon-borne hygrometers exhibits gradual increase in the 1980s and 1990s (Oltmans and Hofmann, 1995; Oltmans et al., 2000) followed by a stepwise drop at around the year 2000 (Scherer et al., 2008; Fujiwara et al., 2010). Since SWV has a positive radiative forcing as a greenhouse gas (Shindell, 2001), its possible increase during the two decades could have caused enhanced surface warming by about 30 % as compared to that without taking this increase into account, while the subsequent drop could have slowed down the surface warming by about 25 % from about 0.14 to 0.10 °C per decade (Solomon et al., 2010). The cause and mechanism of this stepwise change have been fluently discussed (e.g., Randel et al., 2006; Rosenlof and Reid, 2008; Bönisch et al., 2011; Fueglistaler, 2012; Fueglistaler et al., 2014; Dessler et al., 2014). While constructing a reliable long-term SWV record is still a challenge (Hegglin et al., 2014), the understanding of a possible stepwise change in SWV is required in assessing possible modulation of the Brewer–Dobson circulation under global warming.

The variation of SWV is driven dynamically by the troposphere-to-stratosphere transport of water and chemically by the oxidation of methane. The dynamical control is mostly associated with the efficiency of dehydration functioning on the air mass advected in the TTL (Holton and Gettelman, 2001; Hatsushika and Yamazaki, 2003). The Lagrangian description of the transport processes in the tropical troposphere to the stratosphere using trajectory calculations proved to be quite effective not only in the reproduction of SWV variations but also in the characterization of the dehydration processes in the TTL (e.g., Bonazzola and Haynes, 2004; Fueglistaler et al., 2004, 2005; Dessler et al., 2014) even though the quantitative estimation of the water amount entering the stratosphere requires detailed consideration dealing with aerosols and ice particles (ice nucleation and sublimation processes, supersaturation, and deposition and precipitation of ice particles) as well as the minute description of meteorological conditions (subgrid-scale variabilities, intrusion of deep convection into advected air parcels, and irreversible mixing due to breaking waves along with the ambiguity in the analysis field).

Here, we discuss the cause of the stepwise drop in SWV by making the analysis of the entry mixing ratio of water to the stratosphere ($[H_2O]_e$) with the aid of some Lagrangian diagnostics of TTL dehydration such as the preferred advection pathways in the TTL, the location in which water saturation mixing ratio (SMR) takes minimum along each trajectory (Lagrangian cold point; LCP)

together with the minimum value (SMR_{min}) before entering the stratosphere (Sect. 3). The backward kinematic trajectories initialized on 400 K potential temperature surface in the tropics, similar to those of Fueglistaler et al. (2005), are used. The calculations cover the period from January 1997 to December 2002. The statistical features of the LCP and SMR_{min} are analyzed for the 90 day trajectories in which the air parcels experienced LCP in the TTL (Sect. 2). The analysis is focused on the examination of the entry value of water to the stratosphere, meaning that any contribution from the recirculation within the stratosphere (ST) and the sideway entry of water to ST without taking the LCP in the TTL are intentionally left out of the scope. Detailed examinations on the driving mechanism itself are left for future studies. However, such a restriction will serve to focus our investigation on some specific processes that may have led to the SWV drop in Lagrangian framework. This approach has an advantage over Eulerian description because the drop in SWV does not necessarily mean TTL cooling conveniently described in Eulerian framework. For example, it might simply reflect the change in the proportion of air parcels that have passed the coldest region in the TTL. Conversely, any extreme cooling does not necessarily result in enhanced dehydration as long as the air parcels do not experience LCP event in that region. We will try to describe a hypothetical story on the cause of the stepwise drop of SWV through the discussion of the results in Sect. 4. Conclusions are placed in Sect. 5.

2 Method of analysis

2.1 Trajectory calculations

The method of estimating $[H_2O]_c$ in the present study is similar to that of Fueglistaler et al. (2005). $[H_2O]_c$ at time t is estimated as the ensemble mean value of SMR_{min} along 90 day backward kinematic trajectories initialized at t. The backward trajectory calculations are started from uniformly distributed gridpoints (every 5.0° longitude by 1.5° latitude) within 30° N and S from the equator on 400 K potential temperature surface. The initializations are made on the 5th, 15th, and 25th of every month during the period since January 1997 till December 2002 relying on the European Centre For Medium-Range Weather Forecasts ERA Interim dataset (Dee et al., 2011). The number of initialization points is 2952 for a single calculation resulting in 8856 for the estimation of monthly values. This number compares well with that of the reduced set of trajectories in the study on the sensitivity of number of trajectories by Bonazzola and Haynes (2004) and turned out to be enough to derive statistically significant results as can be seen later in Section 3. All meteorological variables given on 60 model levels have been interpolated to those on 91 pressure levels keeping the horizontal resolution of 0.75° by 0.75° longitude–latitude gridpoints prior to calculations. The time step has been set to 30 minutes, similar to 36 minutes taken by Bonazzola and Haynes (2004), by applying spatiotemporal interpolations to the 6-hour interval ERA Interim dataset. As for the limitation and

caution of this method, see, for example, the pioneering studies by Fueglistaler et al. (2004) and Bonazzola and Haynes (2004).

2.2 Selection of trajectories relevant to TTL dehydration

The meridional projections of the backward trajectories extracted from those initialized on 15 January 1999 are shown in Fig. 1. The top and bottom diagrams are the same except that pressure (top) and potential temperature (bottom) are taken as the ordinate. The asterisks in red indicate the location of the LCP while those in green are the termination point of trajectory calculations (90 days before initialization at the longest). In case the backward extension of the trajectories hit the surface of the earth, the calculations are terminated at that point, and those portions of the trajectories immediately before the surface collision are used for the analysis. The migration of air parcels depicted in the trajectories is roughly categorized into three major branches: quasi-isentropic advection in the TTL and the lower stratosphere (LS), vertical displacement in the troposphere due to diabatic motion resolvable in grid-scale velocity field, and quasi-isentropic migration in the troposphere. We can see many air parcels are traced back to the troposphere representing the tropical troposphere-to-stratosphere transport (TST), while some portion of the trajectories remain in the LS and/or reach the tropical 400 K surface by taking the sideways without making excursions in the TTL. All non-TST trajectories are removed from the following analysis to focus our discussion on the modulation of $[H_2O]_c$. For the sake of clarity, the TST particles in the present study are defined as a subset of those particles traceable down to 340 K having recorded LCP in the TTL. For the application of this LCP condition to our trajectories, we introduce the Lagrangian definition of the TTL to assure internal consistency of the analysis.

The motion of air parcels ascending in the tropical troposphere is characterized by rapid convective up-lift that accompanies latitudinal migration associated with the seasonal displacement of the Inter-Tropical Convergence Zone. Up in the TTL, on the other hand, the diabatic ascent is driven by radiative heating, in which the seasonal migration with respect to latitude is much smaller than that in the troposphere because the dynamical field generated by the thermal forcing at the bottom boundary retains relatively high symmetry with respect to the equator. By translating these features into the characteristics of trajectories, we derive a definition of the TTL in a Lagrangian fashion.

Figure 2 on the top illustrates the vertical distribution of the proportion of trajectories categorized on a daily basis as "fast" ascending air parcels. The required rate for the fast ascent is empirically set to more than 0.2 K in potential temperature within 1 time step (30 min), that is, the condition for θ K isentrope is met if the air parcel crosses θ K surface from below $\theta - 0.1$ K to above $\theta + 0.1$ K in 30 min. We can see that the proportion of the fast diabatic ascent thus defined takes maximum at around 340 K in the troposphere and minimum at around 355 K. The proportion of such "fast" air parcels reduces above the level of main outflow and rapidly goes to near zero toward the level of zero net radiative heating in the TTL. Above this level, the air parcels are diabatically lifted

up by radiative heating and further pumped-up by dissipating planetary waves in the midlatitude stratosphere (Holton et al., 1995). The alternation of the primary forcing that drives diabatic ascent is also seen from the bottom panel of Fig. 2, which shows the seasonal migration of the latitudinal position of the trajectories traceable to down below 340 K averaged for (blue) January, (green) April, (yellow) July, and (red) October. The altitude of the kink at around 355 K suggests that the influence of tropical convective motion almost ceases at this level and the diabatic forcing gradually shifts to radiative heating in the TTL and above.

The diagnostic features depicted in Fig. 2 agree that the bottom of the TTL would be most properly defined at 355 K potential temperature level for our study. In the following analysis, we make use of TST trajectories defined by the air parcels that have ascended from the lower troposphere below 340 K isentrope experiencing the LCP in the TTL, which is defined by the layer between the isentropic levels 355 and 400 K within 30° N and S from the equator.

3 Results

3.1 The drop in $[H_2O]_e$

The calculations are made on a monthly basis using the three initialization days (5th, 15th and 25th of each month) at a time. The following description refers to a specific month omitting the suffix for time. Let start by assuming that the minimum saturation mixing ratio along i-th TST trajectory ($i = 1, \cdots, N_{\mathrm{TST}}$) is denoted by $\mathrm{SMR}_{\mathrm{min}\,i}$. The entry value of water to the stratosphere $[H_2O]_e$ is defined as the ensemble mean value of $\mathrm{SMR}_{\mathrm{min}}$ as in Fueglistaler et al. (2005):

$$[H_2O]_e = \frac{1}{N_{\mathrm{TST}}} \sum_{i}^{N_{\mathrm{TST}}} \mathrm{SMR}_{\mathrm{min}\,i}. \quad (1)$$

The evolution of the entry value of water to the stratosphere as modeled in $[H_2O]_e$ time series is shown in Fig. 3. The top panel is the sequential change in the monthly ensemble mean value of $[H_2O]_e$ estimated from the TST air parcels during the period between January 1997 and December 2002. We can see the decrease of the seasonal maxima in boreal summer in 2000. The seasonal minima in boreal winter, on the other hand, show larger values in January–February 2000 as compared to those in 1999, 2001, and 2002 and thus the drop in $[H_2O]_e$ is not quite obvious. As the six-year time series is not long enough to define climatology and anomalies from it, we simply view the interannual variations on the basis of each calendar month. The bottom panel of Fig. 3 is the same as the top except that the data points are connected by each calendar month. When viewed in this way, the drop in the year 2000 of about 1 ppmv shows up in the time change in September (marked by 9), October (10), November (11), and December (12). Similar drop continues to January (1) and the successive months in 2001. As there is little difference between those in August 1999 and 2000, we may well conclude that the drop in $[H_2O]_e$ occurred in September 2000. Considering the time period required for the air parcels to make excursion in the TTL, we may interpret that the change

in the characteristics of dehydration has been initiated in the boreal summer of 2000. The maxima of $[H_2O]_e$ in January through June 1998 are related to the strong El Niño as is discussed later in Sect. 4.

3.2 Horizontal projection of the TST trajectories

As the first step of examining the change in the characteristics of TTL dehydration initiated in northern summer of 2000, Fig. 4 illustrates the horizontal projection of TST trajectories within the layer between the isentropes 360 and 370 K extracted from those initialized in September 1999 (top) and 2000 (bottom). In spite of the equatorially symmetric assignment of the initialization points on 400 K potential temperature surface, the trajectories in the TTL are highly asymmetric with respect to the equator and clustered mostly in the northern subtropics. The dense population of the trajectories shows that the air parcels are largely trapped by Tibetan high in the region between 30° W to 150° E and 0 to 45° N. Comparison between the two, representing September trajectories prior and posterior to the drop, respectively, reveals that the circulation of air parcels around the Tibetan high is loosely tied to the center in the latter period, resulting in the expansion of the anticyclonic circulation branch mostly to the east accompanied by the spread-out of the trajectories farther to the Southern Hemisphere in the latter. This modal shift in the trajectories initialized in September occurs in the year 2000 and continues at least through 2001 and 2002 (not shown).

3.3 Statistical distribution of the LCP

The shift in the circulation pattern of air parcels is not enough to characterize the modification of dehydration efficiency in the TTL. To quantify the change in the LCP distribution associated with the modal shift seen in Fig. 4, the numbers of LCPs are counted by every 10° longitude-latitude bin in the tropics. The probabilities of LCPs are estimated for each bin by dividing the LCP counts by the total number of TST trajectories.

Let assume that i-th TST trajectory ($i = 1, \cdots, N_{\mathrm{TST}}$) takes minimum saturation mixing ratio ($\mathrm{SMR}_{\mathrm{min}\,i}$) at bin j ($j = 1, \cdots, M$), that is, the Lagrangian cold point (LCP) for i-th TST trajectory is found at bin j. If we denote the number of LCP events at bin j as $N(\mathrm{LCP} \in j)$,

$$N_{\mathrm{TST}} = \sum_{j}^{M} N(\mathrm{LCP} \in j). \tag{2}$$

Because some trajectories do not satisfy the TST condition in general, $N_{\mathrm{TST}} \leq N$, where N is the total number of initialization points used for the calculation. The probability of LCP events at bin j, $P(\mathrm{LCP} \in j)$, is defined by

$$P(\mathrm{LCP} \in j) = \frac{N(\mathrm{LCP} \in j)}{N_{\mathrm{TST}}}, \tag{3}$$

so that the normalization condition $\sum_{j}^{M} P(\mathrm{LCP} \in j) = 1$ holds.

The top two panels of Fig. 5 show the horizontal distributions of $P(\mathrm{LCP} \in j)$ thus defined for those trajectories initialized in September 1998 and 1999 (a; prior to the drop) and September 2000, 2001 and 2002 (b; posterior to the drop). Because N_{TST} is different among individual September, N_{TST} for each month has been used as a weight in taking the averages. In other words, the calculations are made by combining the trajectories of two or three prior- or posterior-months together for the illustrations. To be more specific, the TST trajectories of September 1998 and 1999, selected from $N = 2952 \times 3 \times 2$ trajectories, are combined together for the illustration of Fig. 5(a), while those of September 2000, 2001, and 2002, selected from $N = 2952 \times 3 \times 3$ trajectories, are used for Fig. 5(b). The comparison between the two will shed light on the change in "the sampling effect" of Bonazzola and Haynes (2004). The spatial distribution is characterized by the maxima over the Bay of Bengal and Malay Peninsula accompanied by a ridge extending to South China Sea. It is interesting to note some similarity in the location to the spatial maxima of the first encounter of backward trajectories to 370 K isentrope for June to August 1999 shown by Bonazzola and Haynes (2004). During the period posterior to the drop (Fig. 5(b)), the maxima show eastward expansion as far as 150° E. There also appears some increase in the Central Pacific covering both northern and southern subtropics crossing over the equator. These two components appear clearer in the difference field shown in Fig. 5(c). Those bins shown in blue (red) indicate the decrease (increase) of the LCP probabilities in the posterior period. The test statistic of the difference (see Appendix A1 for details) is shown in Fig. 5(d) indicating the region in which the differences are statistically significant at the significance level of 1 % or higher. It is interesting to note that, in addition to the dipole structure associated with the eastward expansion of the Tibetan anticyclone, the probabilities show significant decrease over the equator at around 130 to 140° E and increase in wider area almost symmetric with respect to the equator (160° E to 160° W and 10° S to 10° N). This structure will be discussed further in Sect. 4.

3.4 Statistical change in the $\mathrm{SMR}_{\mathrm{min}}$

The increase of the LCP events in some bins does not necessarily mean enhanced dehydration over there. The next step is to examine the change in the $\mathrm{SMR}_{\mathrm{min}}$. This corresponds to focus on the change in "the temperature effect" of Bonazzola and Haynes (2004). Simultaneous with counting the LCP events, the values of SMR at the time of each LCP event ($\mathrm{SMR}_{\mathrm{min}}$) have been summed-up to calculate the average for each bin. The ensemble mean value of $\mathrm{SMR}_{\mathrm{min}}$ at bin j, SMR(LCP$\in j$), is defined by

$$\mathrm{SMR}(\mathrm{LCP} \in j) = \frac{1}{N(\mathrm{LCP} \in j)} \sum_{i}^{\mathrm{LCP}\in j} \mathrm{SMR}_{\mathrm{min}\,i}, \tag{4}$$

where $\sum_{i}^{\mathrm{LCP}\in j}$ indicates the sum with respect to the subset of TST trajectories that take LCP at bin j.

Figure 6 is the same as Fig. 5 except that SMR(LCP$\in j$) is illustrated rather than $P(\mathrm{LCP} \in j)$. We can see that the averages of $\mathrm{SMR_{min}}$ in the tropics are roughly smaller in the eastern than in the western hemisphere accompanying a broad minimum of about 3.5 to 3.7 ppmv over the maritime continent during the period prior to the drop (Fig. 6(a)). The values show general decrease in the tropics with some enhanced drop in the central Pacific reaching less than 3.0 ppmv in the period posterior to the drop (Fig. 6(b)). The gross features correspond well to the horizontal distribution of the LCP-averaged SMR of July/August 2001 estimated by Fueglistaler et al. (2004). The difference between the two periods (Fig. 6(c)), together with the statistical significance (Fig. 6(d)), confirms the pronounced decrease of $\mathrm{SMR_{min}}$ in the central Pacific after 2000. On the other hand, the change of $\mathrm{SMR_{min}}$ associated with the east-west dipole structure is not so remarkable in terms of the difference of $\mathrm{SMR_{min}}$, although the tendency is the same.

3.5 Statistical change in the expectation values

While the differences of $\mathrm{SMR_{min}}$ appear smaller over the Bay of Bengal and Malay Peninsula than over the central Pacific, the comparisons based only on the changes in SMR(LCP$\in j$) could be misleading, because the values of $P(\mathrm{LCP} \in j)$ are much higher in the former than in the latter (Fig. 5). The expectation value for bin j, $E(\mathrm{LCP} \in j)$, is defined by the multiple of $P(\mathrm{LCP} \in j)$ and SMR(LCP$\in j$) to quantify the contribution of each bin to $[\mathrm{H_2O}]_e$. The sum of $E(\mathrm{LCP} \in j)$ with respect to all bins reduces to

$$\sum_j^M E(\mathrm{LCP} \in j) = \sum_j^M P(\mathrm{LCP} \in j) \times \mathrm{SMR}(\mathrm{LCP} \in j) \quad (5)$$

$$= \sum_j^M \frac{N(\mathrm{LCP} \in j)}{N_{\mathrm{TST}}} \times \frac{1}{N(\mathrm{LCP} \in j)} \sum_i^{\mathrm{LCP}\in j} \mathrm{SMR}_{\mathrm{min}i} \quad (6)$$

$$= \frac{1}{N_{\mathrm{TST}}} \sum_j^M \sum_i^{\mathrm{LCP}\in j} \mathrm{SMR}_{\mathrm{min}i} \quad (7)$$

$$= \frac{1}{N_{\mathrm{TST}}} \sum_i^{N_{\mathrm{TST}}} \mathrm{SMR}_{\mathrm{min}i}. \quad (8)$$

This is the entry value of water to the stratosphere $[\mathrm{H_2O}]_e$ (Eq. (1)) shown as a time series in Fig. 3. $[\mathrm{H_2O}]_e$ is thus decomposed of the sum of $E(\mathrm{LCP} \in j)$, which is interpreted as the contribution of bin j to $[\mathrm{H_2O}]_e$. What is important here is that it is neither $P(\mathrm{LCP} \in j)$ nor SMR(LCP$\in j$) but the product between the two, $E(\mathrm{LCP} \in j)$, that is directly responsible for composing the value $[\mathrm{H_2O}]_e$. By comparing the distribution of $E(\mathrm{LCP} \in j)$ between the two periods, prior and posterior to the drop, we can see how the drop in $[\mathrm{H_2O}]_e$ is brought about by the change of water transport from individual region.

Figure 7 shows the horizontal distribution of $E(\mathrm{LCP} \in j)$. This corresponds to the projection of $[\mathrm{H_2O}]_e$ onto each bin. We can see that the September values of $[\mathrm{H_2O}]_e$ are mostly projected to the

Bay of Bengal and Malay Peninsula before the drop (Fig. 7(a)). The contribution from this core area remains dominant during the posterior period (Fig. 7(b)). While the reduction of $[H_2O]_e$ cannot be free from the general cooling (lowering of SMR(LCP$\in j$)) in posterior years over most of the tropics (Fig. 6), it is interesting to note the increase of $E(\mathrm{LCP} \in j)$ despite the decrease in SMR(LCP$\in j$) over the central Pacific. This is because the increase of $P(\mathrm{LCP} \in j)$ more than compensate for the decrease of SMR(LCP$\in j$) over there. In this sense, it is not appropriate to attribute the cooling over the western and the central Pacific to the drop in $[H_2O]_e$. The similarity in the spatial distributions of $P(\mathrm{LCP} \in j)$ and $E(\mathrm{LCP} \in j)$, especially that of the location of maxima over the Bay of Bengal and Malay Peninsula together with the post 2000 decrease over there and the western tropical Pacific, suggests that the relocation of LCPs (change in $P(\mathrm{LCP} \in j)$) is a leading factor that has caused the drop in $[H_2O]_e$ in September 2000.

The resultant changes could be interpreted as the composite of two components: (i) the decrease over the Bay of Bengal and (ii) the decrease over the equatorial western Pacific and the increase over the central Pacific almost symmetric with respect to the equator extending to the subtropical latitudes of both hemispheres. The former is supplemented by slight decrease widespread along the 10° N zonal belt with the exception around 150° E and the central Pacific. These features will be related to the eastward expansion of the anticyclonic circulation around the Tibetan high, while the latter is suggestive of some response to the thermal forcing from the equatorial ocean.

4 Discussion

4.1 Maxima of $[H_2O]_e$ in 1998

We have seen in Fig. 3 that the time series of $[H_2O]_e$ shows maxima in January through June 1998. We excluded these months from our analysis in Sect. 3 because of the influences of strong El Niño. The values of $[H_2O]_e$ in November and December 1997 are larger than those in 1998, which may suggest possible influence of El Niño also in these months. Actually Fueglistaler and Haynes (2005) demonstrated in their Fig. 2 that the trajectory model shows large increase of lower-stratospheric water ($[H_2O]_{T400}$ which takes non-TST trajectories into account in addition to $[H_2O]_e$) associated with El Niño and that the increase is accompanied by the eastward shift of the high density region of LCP. The reason why we regard these facts as little related to the drop of $[H_2O]_e$ in 2000 is briefly discussed here.

For exploration of the reason of such anomalies, the horizontal distributions of LCP are shown for those initialized in February 1997, 1998 and 1999 in Fig. 8. The distributions in February 2000, 2001 and 2002 (not shown) are similar to those of 1997 and 1999. The LCPs in February are commonly distributed almost symmetric with respect to the equator, but the longitudinal distribution is not uniform. High concentration in the western tropical Pacific in 1997 and 1999 (and also in 2000, 2001 and 2002) is suggestive of the strong influence of the warm sea surface temperature (SST) on

the LCP distribution. The large scatter extending to the eastern tropical Pacific in 1998 is due to the migration of the large scale convective system to the east associated with the strong El Niño. We have put this anomalous change out of the scope of the present study, because those anomalous values seem to have recovered to normal by the northern summer of 1998 (well before 2000) and there is no reasoning that this strong El Niño is coupled to the drop in $[H_2O]_e$ in 2000. For the objective judgement of the influence of the El Niño, we employ the SST averaged in the region between 90° W and 150° W longitude and 5° S to 5° N latitude (Niño 3 region, Trenberth, 1997). Those months exhibiting the SST anomalies (relative to the 1981-to-2010 climatology) greater than 1.5 times the standard deviation are excluded from the present analysis. Those excluded are the twelve months from June 1997 to May 1998.

4.2 Perspective to the mechanism of the drop

The entry value of water to the stratosphere, $[H_2O]_e$, estimated by the ensemble mean values of SMR_{min} along the TST trajectories shows appreciable decrease in September 2000 (Fig. 3), suggesting some modulation in the dehydration efficiency functioning on the air parcels advected in the TTL during the northern summer of 2000. The horizontal projection of September trajectories, characterized by anticyclonic circulation associated with Tibetan high in the TTL, shows eastward expansion in the year 2000 accompanied by some bifurcation to the Southern Hemisphere (Fig. 4). This modal shift appears as decreases in the probability distribution of the LCP over the Bay of Bengal and the western tropical Pacific (Fig. 5). The SMR averaged on the occasion of LCP events (SMR_{min}) shows general decrease with some enhancement in the central Pacific (Fig. 6). These results suggest two possible components contributing to the sudden drop of $[H_2O]_e$ in September 2000: the modulations of the Tibetan high and the TTL circulation driven by the thermal forcing from the equatorial ocean. The regional contribution to $[H_2O]_e$, quantified by $E(\mathrm{LCP} \in j)$, shows distinct decrease in two regions; one over the Bay of Bengal and the other over the equator in the western tropical Pacific (Fig. 7(c)). The former will be related to the weakening of Tibetan high, while the latter may imply the modulation of the Matsuno-Gill pattern (Matsuno, 1966; Gill, 1980), although these will not be independent between each other. The results indicate that the drop is brought about by a response of the TTL circulation to the modulated forcing both from the continental summer monsoon and the equatorial ocean. It is thus quite interesting to take a brief look at the changes in the TTL meteorological fields in Eulerian framework before concluding this study.

Figure 9 illustrates the longitude-latitude section of 100 hPa geopotential height (left) and temperature (right) averaged in August 1998 and 1999 (top) and 2000, 2001 and 2002 (middle). These are the background Eulerian fields having roughly brought about the Lagrangian features described by the top two panels of Figs. 5–7. We can see the Tibetan anticyclone in the height field of both periods (left) with the intensity weaker in the latter (2000, 2001 and 2002) than in the former (1998 and 1999). This feature appears basically the same in individual monthly mean values of August

depending on the category either prior or posterior to the drop. The expansion of the trajectories after 2000 (Fig. 4), therefore, is the result of loosened grip of air parcels around weakened Tibetan high in the latter years. These features remain the same in September of other years posterior to the drop (not shown). The temperature field (right-hand side) both prior and posterior to the drop appears as the typical pattern of the TTL response to the thermal forcing at the bottom boundary with additional heating to the subtropical Northern Hemisphere (Matsuno, 1966; Gill, 1980). The difference (Fig. 9(e)) indicates substantial cooling in the northern subtropics at around 150° E and the central Pacific. The latter corresponds to the findings of Rosenlof and Reid (2008) in which the tropical tropopause temperature in 171 to 200° E longitude band decreased in association with the SWV drop in 2000.

The correspondence of the decrease of the equatorial 100 hPa temperature to the increase of the underlying SST is explored in Fig. 10, which shows the longitude-time section of the equatorial SST averaged between 10° N and S of the equator. We could see the warm SST region in the western Pacific expands to the east in the year 2000, and the contour of 28 °C, the threshold of active convection (Gadgil et al., 1984), during the coldest month of the year crossed the date line in 2001. The possible connection of the water drop in 2000 to the modified SST distribution has been discussed by Rosenlof and Reid (2008). They found the correlation coefficients between tropopause temperature and SST are quite small "if one correlates times prior to 2000, or after 2001" separately, but a large negative correlation coefficient of – 0.44 appears if one correlates the entire time period which, they say, is "exclusively a consequence of the decrease in tropical tropopause temperatures of $\sim 2\,^{\circ}\mathrm{C}$ in 171°–200° longitude band coincident with an increase in SSTs of 0.4 °C in the 139°–171° tropical longitude band." The longitudinal difference between the warm SST core and the temperature minimum near the tropopause will be due to the eastward tilt of cold region associated with a steady Kelvin wave response to underlying convective heating (Hatsushika and Yamazaki, 2003). Thus the notion by Rosenlof and Reid (2008) suggests that the SWV drop in 2000 is driven by some dynamical process that accompanies the generation of Matsuno-Gill pattern. This is consistent with the idea that the modified SST distribution is one of the key processes that drove the water drop in the year 2000. The warm condition in the central Pacific continues at least till the end of 2005. The decrease of 100 hPa temperature over the central Pacific is, thus, well correlated to this SST variation.

The important point in our analysis is that the decrease of SMR(LCP$\in j$), albeit widely distributed and remarkable in the tropics (Figs. 6 and 9), is not enough to explain the drop of $[\mathrm{H_2O}]_e$ if we recognize the dipole structure, that is, the paired increase and decrease, in $E(\mathrm{LCP} \in j)$ over the equatorial Pacific (Fig. 7). The modified pathway of TTL trajectories, resulted in the reduction of LCP probabilities over the Bay of Bengal and the western tropical Pacific (Fig. 5), is quite important.

The study by Young et al. (2012), discussing the changes in the Brewer–Dobson circulation during the period 1979 to 2005 by referring to the out-of-phase temperature relationship between the tropics and the extratropics, found no appreciable change around the year 2000. However, the zonally

uniform component exhibiting the out-of-phase relationship between the tropics and the extratropics in 100 hPa temperature difference (Fig. 9) is suggestive of some stratospheric contribution to the drop in $[H_2O]_e$ (Randel et al., 2006) through wave-driven pumping (Holton et al., 1995). Actually the analysis of dynamical fields such as eddy heat flux and EP-flux by Fueglistaler (2012) finds a strengthening of the residual circulation qualitatively consistent with the drop of SWV in *October* 2000. Figure 11 shows in color the time-height section of monthly mean vertical wind velocity in the tropics. The seasonal enhancement in the upward motion during northern winter shows up in the lowermost stratosphere. The solid and dashed contours superposed on the vertical velocity field are the zonal wind components depicting the westerly and the easterly phase, respectively, of the quasi-biennial oscillation (QBO). The stagnation of the downward propagation specifically that of the easterly phase of the QBO is noticed in late 1997 to early 1998 and late 2000 to early 2001 at around 40 hPa level. This phase dependency of the stagnant propagation is brought about by the secondary circulation of the QBO in which the upward (downward) motion accompanies the easterly (westerly) shear zone of the QBO (Plumb and Bell, 1982; Hasebe, 1994). What is interesting here is that the enhanced upward motion is found in September and October 2000 blocking the downward propagation of easterlies. The limitation from our use of Eulerian vertical velocity, rather than TEM residual velocity, will be minimal as we focus our discussion in the tropics. Actually the anomalies in the equatorial upwelling at 78 hPa estimated by Rosenlof and Reid (2008) show similar results. Further analysis by Fueglistaler et al. (2014) emphasize that the strengthening of the residual circulation does not last long but continues for a few years around the year 2000. Remembering the time of excursion for air parcels circulating the Tibetan high (Fig. 4), the stratospheric anomalies in October 2000 (Fueglistaler, 2012) appears later than the initiation of the drop in $[H_2O]_e$. The difference of one month, albeit small, is large enough to be resolved in the analysis. Then the enhanced upwelling discussed by Fueglistaler et al. (2014) might be the stratospheric response to the tropospheric forcing that modulated the dehydration efficiency in the preceding boreal summer of 2000 rather than the direct cause of the SWV drop. Further studies employing numerical simulations are definitely required. It is worth mentioning here that the enhancement of the Brewer–Dobson circulation may have occurred also in the northern hemispheric branch; the age of northern mid-latitude stratospheric air diagnosed by the CO_2 concentration appears shorter than usual in 2002 (Engel et al., 2009, Fig. 3), although the difference is not statistically significant.

4.3 Perspective to the mechanism of sustained low amount of $[H_2O]_e$

We have seen some background meteorological fields from Eulerian perspective to interpret the evidences presumably responsible for the drop of $[H_2O]_e$ in September 2000 described in Lagrangian framework. The problems not yet answered are what is the specific event (if any) and how is it generated that has triggered the sequence of phenomena that ultimately led to the sudden drop of SWV. In addition, the sustained low values of $[H_2O]_e$ after September 2000 need some mechanism that

lasts longer than the seasonal time scale, since the modulation of Tibetan high cannot explain the reduction continuing to the successive months in northern winter (Fig. 3).

Figure 12 is the same as Fig. 7 except that the January projection is illustrated. We can see, in addition to tbe values generally lower than those in September, the larger values are found in the western tropical Pacific (Fig. 12(a), (b)), indicating the January values of $[H_2O]_e$ are controlled by those over the western Pacific. This is consistent with the picture having been presented in numerical simulations (Hatsushika and Yamazaki, 2003). The difference between the two periods (Fig. 12(c)) shows decrease over Indonesia and increase over the central Pacific during the period posterior to the drop. The former is due to the combination of the decreases in both $P(\mathrm{LCP} \in j)$ and SMR(LCP$\in j$), while the latter is brought about by the interplay between the increase in $P(\mathrm{LCP} \in j)$ and some decrease of SMR(LCP$\in j$) (not shown). This situation is the same as what we see in September (Section 3.5). The similarity of this pattern, that is, the decrease in the equatorial western Pacific (over Indonesia) and the increase over the central Pacific, to that of the second component of September response suggests the existence of a common driver of the drop in $[H_2O]_e$ irrespective of the season. These evidences suggest the idea that the drop of $[H_2O]_e$ in northern winter has resulted from the response of the TTL circulation to the eastward expansion of the warm water to the central Pacific (Fig. 10) in such a way that the decrease of $E(\mathrm{LCP} \in j)$ in the western Pacific exceeds the increase of that in the central Pacific.

The correspondence to the change in the SST distribution, the time of occurrence, and the persistency of phenomenon suggest that the drop and the subsequent low values of $[H_2O]_e$ are brought about by the reduced water entry to the stratosphere mainly through the Bay of Bengal (in boreal summer) and the Western tropical Pacific. The dipole pattern in $E(\mathrm{LCP} \in j)$ over the equatorial Pacific (Figs. 7 and 12) is suggestive of an eastward shift of Matsuno-Gill pattern related to the eastward expansion of warm SST region to the central Pacific. Then our hypothetical story may read, the eastward expansion of warm SST region brings about the reduction of $[H_2O]_e$ by TST air parcels passing through the western tropical Pacific during northern winter (Fig. 12), while the heating from the modulated SST mentioned above, competing against that over the continent, has led to the modal shift of trajectories during northern summer resulting in the reduced water transport over the Bay of Bengal and the western tropical Pacific (Fig. 7).

The above speculation might end up with some proper explanation on the cause of the eastward expansion of the equatorial warm water to the central Pacific observed in 2000. In this context, it is interesting to see possible occurrence of "El Niño Modoki" characterized by the warm SST event over the central Pacific (W. J. Randel, personal communication, 2015). Actually the time series of normalized ENSO Modoki index of Ashok et al. (2007) turns from prolonged negative to positive towards 2001. It is also interesting to note that the "La Niña-like condition," tied to the surface cooling of the equatorial eastern Pacific, is supposedly responsible for the recent hiatus, the pause of the global-mean surface air temperature rise (Kosaka and Xie, 2013; Watanabe et al., 2014). If

proved to be true, we may have unveiled another piece of pathways the internal variability of our climate system could exert on the surface cooling through SST-driven SWV fluctuations.

5 Conclusions

Backward kinematic trajectories, initialized on 400 K potential temperature surface in the tropics, have been employed to describe the stratospheric water drop observed at around 2000 to 2001 from a Lagrangian point of view. The entry value of water to the stratosphere, $[H_2O]_e$, shows appreciable decrease in the trajectories initialized in September 2000 suggesting the change in the TTL dehydration efficiency during the boreal summer of 2000. The following changes are found to be responsible for the drop in $[H_2O]_e$. The reduction of water vapor transported by those air parcels that experienced LCP events in two regions; over the Bay of Bengal and the western tropical Pacific. The reductions are brought about by the decreases in both the LCP-event probability and the ensemble mean SMR_{min} over there. The LCP reduction in the former region is related to the modified migration pathways of air parcels circulating the weakened Tibetan anticyclone, while that in the latter may be a response to eastward expansion of warm water to the central Pacific. This SST modulation seems to be responsible also for the decrease of $[H_2O]_e$ in the successive northern winter. Some indication of stratospheric contribution through intensified pumping appears only intermittent and will be better interpreted as a response to tropospheric forcing changes.

Appendix A: Statistical tests between prior and posterior to the drop

A1 The difference of $P(\mathrm{LCP} \in j)$

Let the random variable, X, is the number of event occurrences in some number of trials, n. The binomial distribution can be used to calculate the probabilities for each of $n+1$ possible values of X $(X = 0, 1, \cdots, n)$ if the following conditions are met: (1) the probability of the event occurring does not change from trial to trial, and (2) the outcomes on each of the n trials are mutually independent. These conditions are rarely met, but real situations can be close enough to this ideal that the binomial distribution provides sufficiently accurate representations. The probability that the number of occurrence X is x among n trials, $\Pr(X = x)$, follows the binomial distribution

$$\Pr(X = x) = \begin{pmatrix} n \\ x \end{pmatrix} p^x (1-p)^{n-x}, \quad (x = 0, 1, \cdots, n), \tag{A1}$$

where p is the probability of occurrence of the event.

The statistical test for the difference in the population proportion of two binomial populations, $p_1 - p_2$, could be made as follows. Let the sample size and the sample proportion of the two sets

being n_1 and n_2 and m_1/n_1 and m_2/n_2, respectively. The test statistic, T_1, defined by

$$T_1 = \frac{m_1/n_1 - m_2/n_2}{\sqrt{p^*(1-p^*)(1/n_1 + 1/n_2)}}, \quad p^* = \frac{m_1 + m_2}{n_1 + n_2}, \tag{A2}$$

follows approximately the standard normal distribution. The statistical test for the difference between $P(\mathrm{LCP} \in j)$ in prior and posterior periods could be done by applying the two-sided tests under the null hypothesis of $p_1 - p_2 = 0$ at some significance level α, where p_1 and p_2 are the population proportion of LCP taking place at bin j in the posterior and prior to the drop, respectively. In our case, n_1 and n_2, and m_1 and m_2, are N_{TST} and $N(\mathrm{LCP} \in j)$, respectively, for posterior (suffix 1) and prior (suffix 2) periods.

A2 The difference of SMR(LCP$\in j$)

The statistical test to be applied is the comparison of the population means of two normal distributions, μ_1 and μ_2, with unknown population variances. This test is sometimes called the Welch's t test. The test statistic, T_2, defined by

$$T_2 = \frac{\overline{x}_1 - \overline{x}_2}{\sqrt{s_1^2/n_1 + s_2^2/n_2}}, \tag{A3}$$

follows the t distribution of the degree of freedom m, where

$$m = \frac{(s_1^2/n_1 + s_2^2/n_2)^2}{s_1^4/(n_1^2(n_1-1)) + s_2^4/(n_2^2(n_2-1))}. \tag{A4}$$

Here, n_1 and n_2, $\overline{x}_1$ and $\overline{x}_2$, and s_1^2 and s_2^2 are the sample size, the sample mean, and the unbiased sample variance, respectively, of the two sets. The statistical test for the difference between SMR(LCP$\in j$) in prior and posterior periods could be done by applying the two-sided tests under the null hypothesis of $\mu_1 - \mu_2 = 0$ at some significance level α. In our case, n_1 and n_2, $\overline{x}_1$ and $\overline{x}_2$, and s_1^2 and s_2^2 are $N(\mathrm{LCP} \in j)$, SMR(LCP$\in j$), and the unbiased variance of $\mathrm{SMR}_{\mathrm{min}}$ at bin j, respectively, for posterior (suffix 1) and prior (suffix 2) periods.

Acknowledgements. This work is based on the Master of Science Thesis of T. Noguchi submitted to the Graduate School of Environmental Science, Hokkaido University in February 2015. T. Noguchi is grateful to the members of the Graduate School of Environmental Science for the encouragement and discussions through the preparation of his thesis. The discussion with Koji Yamazaki of Hokkaido University is greatly appreciated. The results in part have been presented at the CT3LS Meeting having been held in July 2015. F. Hasebe is grateful to the comments from meeting participants especially W. J. Randel of NCAR and K. H. Rosenlof of NOAA. The authors express hearty gratitudes to S. Fueglistaler (referee) and an anonymous reviewer for helpful and constructive comments. NOAA OI SST V2 data are provided by the NOAA/OAR/ESRL PSD, Boulder, Colorado, USA, from their Web site at http://www.esrl.noaa.gov/psd/. This work was supported by the Japan Society for the Promotion of Science, Grant-in-Aid for Scientific Research (S) 26220101.